People's Democratic Republic of Algeria

Ministry of higher education and scientific research

University Amar Telidji Laghouat

Faculty of Sciences

Department of Material Sciences

Field: Physics

Option: Applied Physics

Master thesis presented by:

BAHALIL Messaouda

THEME

On the yet not fully elucidated ground states physical properties of the ternary chalcogenides $AGaS_2$ $(A = K, Rb, Cs)$

Publicly defended before the jury consisting of:

Dr. BOUCHENAFA Mohamed	*President*
Mr. FAID Fares	*Examiner*
Mr. MAABED Said	*Supervisor*

University year 2019-2020

Dedication

This thesis is dedicated to:

The sake of **Allah**, *my Creator and my Master,*

To my father **M'hamed** *who emphasized the importance of education and helped me throughout my life. He is my role-model for hard work, persistence and personal sacrifices; he taught me commitment ,confidence , how to set goals and how to achieve them. He is a man with a vision and good intentions.*

My Mother **Reqaya**; *the unconditional love, taught me that a responsible person who never compromises the quality of life is a person who is capable to make tomorrow better than today; ,and most importantly , I learner from her that t real happiness is to make people happy by lending a hand and thinking of others, thank you.*

My beloved brothers **Mohamed** *and* **Djaloul** *and to my dear sister* **Ouaida**, *also to all my family* **BAHALIL**, *the symbol of love and giving.*

To my supervisor Mr. **MAABED Said**.

To all friends.

To all relatives.

To all neighbours.

All the people in my life who touch my heart.

To all who love me, to everyone I love.

To all those who are dear to me.

Life is a precious gift that we should cherish and invest well; to make it worth living for us and for the generations to come; we must do our best and then; leave the rest to **God**…

I dedicate this work to all of you and prayed **God** *Almighty to be beneficial.*

Messaouda

Acknowlegments

*In the Name of **Allah**, the Most Merciful, the Most Compassionate all praise be to **Allah**, the Lord of the worlds; and prayers and peace be upon Mohamed His servant and messenger.*

*First and foremost, I must acknowledge my limitless thanks to **Allah**, the Ever-Magnificent; the Ever-Thankful, for His help and bless. I am totally sure that this work would have never become truth, without His guidance.*

I owe a deep debt of gratitude to our university for giving us an opportunity to complete this work.

I am grateful to some people, who worked hard with me from the beginning until the completion of the present research particularly my supervisor Mr MAABED Said, who has been always generous during all phases of the research, and I highly appreciate the efforts expended by Mr BOUCHENAFA Mohamed and Mr FAID Fares.

Would also like to thank all the teachers, and a special mention of Mr HALIT Mohamed, Mr HANIFI Mebarki, Mr LEFKAIER Ibn Khaldoun, Mr LAGOUNE Brahim, Mr HELIFA Bachir, Mr KHENCHOUL Salah, Mr CHERIET Abdelrahmane and Mr ARAR Rabie …

I would like to take this opportunity to say warm thanks to all my beloved friends, especilly "El-hamra, Djedia, Fatima, Soumima, Djaouhar, Ouarda, Djouhaina, Hanan, Soumai and Mebarka …" who have been so supportive along the way of doing my thesis.

I also would like to express my wholehearted thanks to my family for their generous support they provided me throughout my entire life and particularly through the process of pursuing the master degree. Because of their unconditional love and prayers, I have the chance to complete this thesis.

Last but not least, deepest thanks go to all people who took part in making this thesis real.

Thank You …

Table of Contents

Chapter III: Results and discussion

List of abbreviations

BZ: Brillouin Zone.

DFT: Density Functional Theory.

DOS: Density of states.

GGA: Generalized Gradient Approximation.

GGA-PBE: Generalized Gradient functional of Perdew-Burk Ernzerhof.

IBZ: Irreducible Brrillouin zone.

LDA: Local Density Approximation.

PDOS: Partial Density of States.

PP: Pseudo-potential.

PW: Plane Wave.

TDOS: Total Density of States.

US-PP: Ultra-soft Pseudo-potentials (Ultra-soft pseudo-potential).

List of tables

Chapter I: Bibliographic review

Chapter III: Results and discussion

List of figures

Chapter I: Bibliographic review

Chapter II: Theoretical framework

Chapter III: Results and discussion

General Introduction

General Introduction

Due to their semiconducting properties and rich chemical structures [1], the ternary chalcogenides $M_xT_yQ_z$ (*M = alkali metal, T = triel, Q = chalcogen*) are interesting materials with admirable physicochemical properties [2].Many of them are known to be semiconductors with gaps varying between 0.9 eV and 4 eV [3, 4]. They crystallize in a large variety of diverse crystal structure types [5]. In this context, the ternary chalcogenides $M_xT_yQ_z$ (*M = alkali metal, T = triel, Q = chalcogen*) have shown a wide range of application in various opto-electronic devices including solar energy converters and light-emitting diodes (LEDs). These materials are also used on a large scale as materials for nonlinear optics (ONL) and detectors [4, 6].

The smallest structural building unit of these compounds are TQ_4 tetrahedra. Condensation of these building blocks yields more complex one, two- or three-dimensional poly-anionic units, which are embedded in a cationic surrounding of the alkali metal cations. The MTQ_2 phases are known for almost all possible element combinations. The dominating structure type among these solids is the $TlGaSe_2$ structure type [7], featuring anionic layers ${}^2_\infty[T_4Q_8^{-4}]$, which seems to have a very high tolerance for different combinations of the elements involved. Another possible anionic substructure of these $M_xT_yQ_z$ phases are anionic chains ${}^1_\infty[TQ_2^-]$ as found in the Tl_2Se_2 [8] and $KFeS_2$ structure types [9].

The present investigation is aimed to report on the hitherto unexplored physical properties of the chalcogenides $AGaS_2$ *(A=K, Rb, Cs)*. Particular attention is paid to investigate their structural, electronic and optical properties using first-principles calculations in the framework of density functional theory (DFT). The manuscript is organized as follows:

In the first chapter, the notion of the $A^IB^{III}C_2^{VI}$ type of compounds is introduced in a general way. Then a short review on the crystallographic structure of the herein considered materials is given.

In the second chapter, we describe the fundamental mathematical aspects of the theoretical background used to solve the many-body quantum mechanics for a system of interacting nuclei and electrons. Of particular interest, the density functional theory (DFT) developed by Kohn-Sham will be outlined in this chapter. In addition, we will introduce some commonly used approximations (GGA, LDA) to deal with the unknown exchange correlation energy, making hands-on a DFT calculation. Some other practical

aspect of DFT such as the plane waves (PW) and pseudo-potential (PP) implementations will be discussed. At the end of the chapter we describe the DFT as implemented in the Cambridge Sequential Total Energy Package (CASTEP), which is used in the present study to calculate all the aforementioned properties of $AGaS_2$ (*A=K, Rb, Cs*) compounds.

The last chapter is devoted to present and discuss the obtained results of $AGaS_2$ (*A=K, Rb, Cs*) compounds.

Finally, a brief conclusion is given summarising the most relevant aspects of obtained results.

References

[1] Huang, F. Q. Deng, B. Ellis, D. E. and. Ibers J. A, "Preparation, structures, and band gaps of $RbInS_2$ and $RbInSe_2$," Journal of Solid State Chemistry, 2005. Vol. 178, pp. 2128-2132.

[2] Zondy, J.-J et al., Frequency doubling of CO_2 laser radiation at 10.6 μm in the highly nonlinear chalcopyrite $LiGaTe_2$. Optics letters, 2007. 32(12): p. 1722-1724.

[3] Reshak .A and Khan .W, "The density functional study of electronic structure, electronic charge density, linear and nonlinear optical properties of single crystal alpha-$LiAlTe_2$,"Journal of Alloys and Compounds, 2014.Vol. 592, pp. 92-99.

[4] Kim .J and Hughbanks .T, "Synthesis and Structures of New Ternary Aluminum Chalcogenides: $LiAlSe_2$, α-$LiAlTe_2$, and β-$LiAlTe_2$," Inorganic Chemistry, 2000.Vol. 39, pp. 3092-3097.

[5] Krebs, B., Thio-und Selenoverbindungen von Haupt gruppenelementen-neue anorganische Oligomere und Polymere. Angewandte Chemie, 1983. 95(2): p. 113-134.

[6] Negran .T, Kasper .H, and Glass .A, "Pyroelectric and electrooptic effects in $LiInS_2$ and $LiInSe_2$,"Materials Research Bulletin, 1973.Vol. 8, pp. 743-748.

[7] Müller, D, Poltmann F.E, and Hahn .H, Zur Struktur ternarer Chalcogenide des Thalliums mit Aluminium, Gallium und Indium, XXII*/On the Structure of Ternary Thallium chalcogenides with Aluminium, Gallium and Indium, XXII. Zeitschrift für Naturforschung B, 1974. 29 (1-2): p. 117-118.

[8] Ketelaar, J., et al., The crystal tructure of TlSe, thallous thallic or thallosic selenide. Zeitschrift für Kristallographie-Crystalline Materials, 1939. 101(1-6): p. 396-405.

[9] Boon, J. and C. Mac Gillavry, The crystal structure of potassium thioferrite $KFeS_2$ and sodium thiochromite $NaCrS_2$. Recueil des Travaux Chimiques des Pays-Bas, 1942. 61(12): p. 910-920.

Chapter I

Bibliographic review

I.1 Introduction

The complex compounds in the $A^I B^{III} C^{VI}$ systems are known to be promising materials for advanced technology, where (A^I - *Li, Na, K, Rb, Cs, Cu, Ag;* B^{III} - *Ga, In, Tl;* C^{VI} - *S, Se, Te*). The ternary compounds provide a number of benefits in comparison with single elements and binary compounds. Especially, compounds of the $A^I B^{III} C_2^{VI}$ type are known to be promising semiconductor, electro-optic, and nonlinear-optical materials [1, 2]. Many of these compounds, particularly those containing alkali metals, have not yet been investigated and those that have been synthesized, have been sparsely studied due to technical difficulties in producing compounds of the $A^I B^{III} C_2^{VI}$ type in the individual state. Besides, prepared samples of these compounds by exchange reactions contain 2 wt. % of oxygen and synthesis from the constituent elements is difficult due to the high chemical reactivity of the alkali metals [3].

The crystal structures of the $A^I B^{III} C_2^{VI}$ type of compounds can be classified into three crystal structural types, derivatives from *ZnS*, *NaCl*, and *TlSe* crystal structural types [4].The $A^I B^{III} C_2^{VI}$ systems (A^I - *Li, Na, K, Rb, Cs;* B^{III} - *Al, Ga, In;* C^{VI} – *S, Se, Te*) viewed through the Periodic Table [Figure I .1].

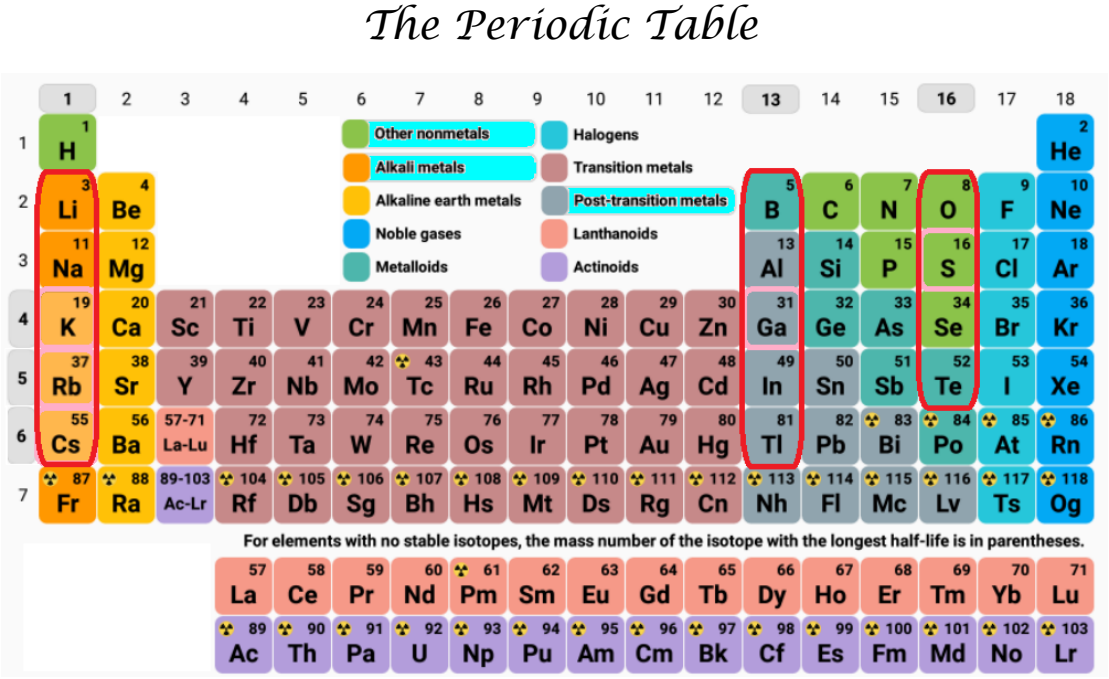

Figure I .1: *The periodic table*

I.2 Formations of the ternary compounds

An overview of the already known ternary compounds of the group 13 metals with chalcogens and alkali metals is given in **Figure I .2**.

The basic building block of the anionic structure, triel cation occurs in most cases, coordinated tetrahedral by chalcogens. The most common exception to the rule is In^{3+}cation, which occurs similarly frequently in octahedral and tetrahedral environments with a similar frequency. The condensation of these TQ_4 tetrahedral (T = triel, Q = chalcogen) at common corners and edges creates complex anions.

Due to the great variety of resulting crystal structures, it is necessary to sort the known structures of the known ternary compounds $M_xT_yQ_z$ (M = *Li, Na, K, Rb, Cs; T = Al, Ga, In; Q = S, Se, Te*) of the alkali metal - triel - chalcogen systems [see **Figure I .2**] according to certain criteria. However, since the only known overview of these compounds from Bernt Krebs from *1983* [5] is mainly about borates and the number of connections has increased very sharply within the last *33* years, it is necessary to sort the known structures of the compounds $M_xT_yQ_z$ according to certain criteria. For this aim, the known connections here are mainly arranged according to the dimensionality of the anion structure.

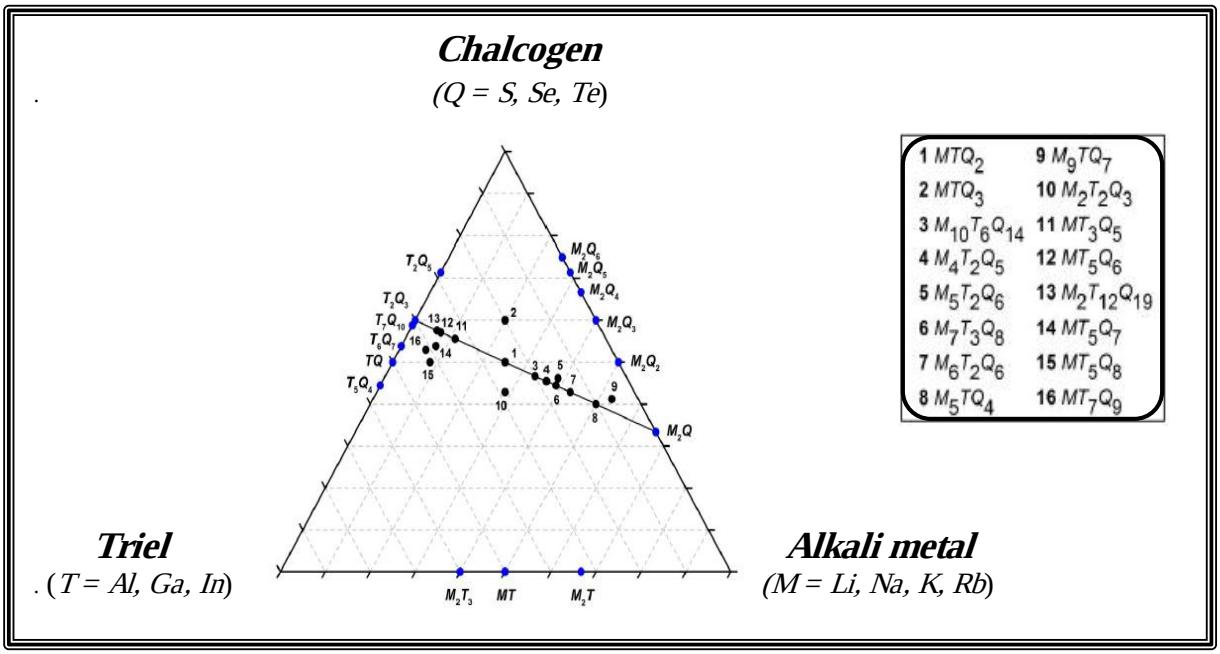

Figure I .2: Ternary phase diagram of alkali metal - triel - chalcogen with the compositions known at the beginning (black points) and the most important binary phases (blue points). The M_2Q-T_2Q_3 conode is also highlighted.

I.3 The crystallographic classification of the $A^I B^{III} C_2^{VI}$ type compounds

The crystallographic classification of the $A^I B^{III} C_2^{VI}$ type compounds is presented in **Figure I .3**

Figure I .3: *The crystallographic classification of the $A^I B^{III} C_2^{VI}$ type compounds.*

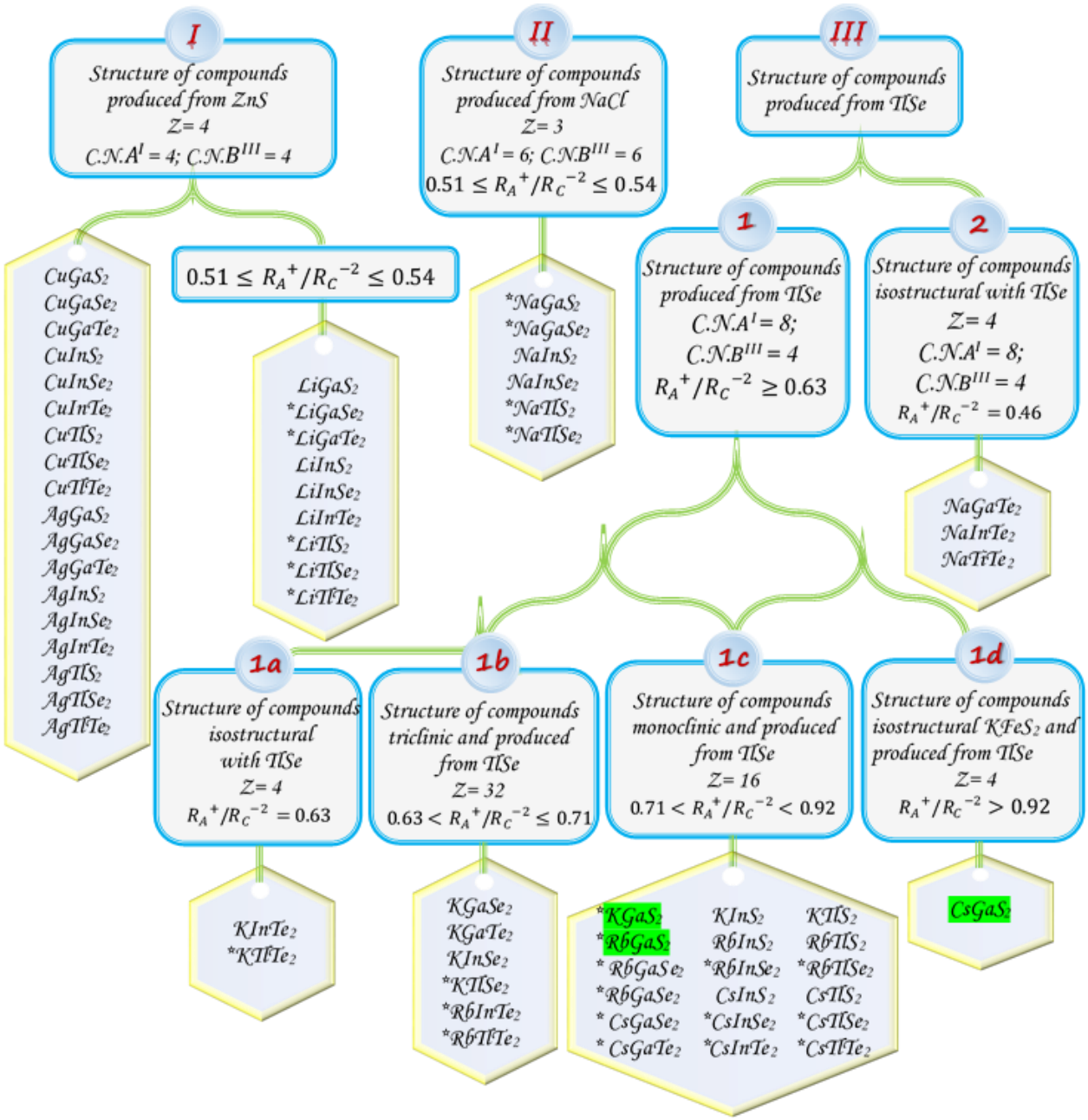

***** - The asterisk indicates the compounds have not been investigated yet.

Z - The number of formula units.

C.N. - The coordination number.

I.4 The crystalline structure of $CsGaS_2$, $KGaS_2$ and $RbGaS_2$

The chalcoginide $AGaS_2$ (A = *K, Rb, Cs*), crystallize in the structure monoclinic (of space group C 2 / c, N °: 15), and the multiplicity of the cell is (Z = 16 for $KGaS_2$, $RbGaS_2$ and Z=4 for $CsGaS_2$). Its asymmetric unit contains two crystallography independent alkaline metal atoms, two independent Gallium atoms and five independent Sulphur atoms. Both polymorphs of $CsGaS_2$ form air and moisture stable colourless crystals. The low-temperature polymorph $CsGaS_2$-*mC64* crystallizes in the $TlGaSe_2$ structure type [5] like many related compounds MTQ_2 (*M = Na, K, Rb, Cs, Tl*; *T = Al, Ga, In*; *Q = S, Se, Te*). The crystal structure of the layered compound features poly-anionic layers $^{2}_{\infty}[Ga_4S_8^{-4}]$, composed of corner-sharing Ga_4S_{10} supertetrahedra. Whose vertices are occupied by Sulphur atoms and the centred by Gallium atoms. These tetrahedra are linked to each other by one of their vertices.

The structural parameters of these three compounds ($KGaS_2$, $RbGaS_2$ and $KGaS_2$) are summarized in **Table I.1**, and monoclinic Structure (*C 2/c*) of $AGaS_2$ (*A=K, Rb, Cs*) are presented in **Figure I .4**.

Figure I .4: *Monoclinic Structure (C 2/c)* of $AGaS_2$ *(A=K, Rb, Cs).*

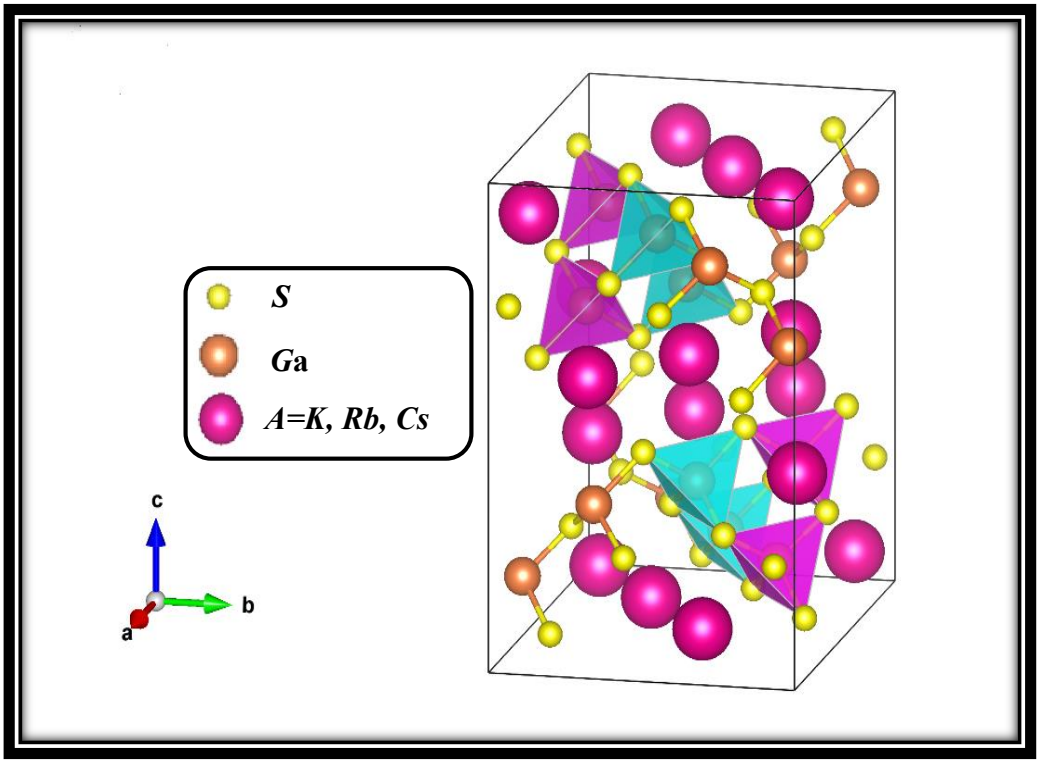

Table I.1: Unite cell parameters and the atomic coordinates of $KGaS_2$, $RbGaS_2$ and $CsGaS_2$.

A= K; Rb; Cs

a: [6]; b: [7]; c: [8].

Lattice parameters (Å)	System								
	$KGaS_2$[a]			$RbGaS_2$[b]			$CsGaS_2$[c]		
a	10.42500			10.48400			10.82910		
b	10.44240			10.46800			10.82920		
c	14.79100			15.39000			16.35910		
$\alpha = \gamma$	90°			90°			90°		
β	100.16°			99.69°			99.44°		
Atomic positions	x	y	z	x	y	z	x	y	z
A1	0.46500	0.31200	0.10900	0.46320	0.18740	0.10620	0.28710	0.06210	0.39970
A2	0.28500	0.06300	0.39000	0.28580	0.43850	0.39520	0.46290	0.31260	0.10260
Ga1	0.10200	0.18900	0.16300	0.10270	0.31060	0.16740	0.10390	0.18920	0.17190
Ga2	0.14500	0.43600	0.33800	0.14380	0.06420	0.33280	0.14270	0.43570	0.32830
S1	0.00000	0.06000	0.25000	0.25420	0.18780	0.25020	0.04070	0.31230	0.41510
S2	0.00000	0.57000	0.25000	0.20800	0.43750	0.08000	0.20970	0.06280	0.08900
S3	0.19900	0.06200	0.07600	0.00000	0.44260	0.25000	0.25270	0.31230	0.25030
S4	0.25500	0.31000	0.25000	0.50000	0.43240	0.25000	0.00000	0.05980	0.25000
S5	0.04500	0.31300	0.43200	0.04360	0.18770	0.42390	0.00000	0.56490	0.25000

I.5 Applications

The $A^I B^{III} C_2^{VI}$ systems (A^I: *Li, Na, K, Rb, Cs, Cu, Ag;* B^{III}:*Al, Ga, In, Tl;* C^{VI} : *S, Se, Te*) have taken a great importance as they can be used in several technologies such as: non-linear optics, electro-optic, light emitting diodes, semiconductors and pyro-electro materials [1, 2].

It is therefore important to study their unexplored physical properties to deduce new potential applications.

I.6 Conclusion

In this chapter, we give a brief description of the $A^I B^{III} C_2^{VI}$ systems and the crystalline structure of $CsGaS_2$, $KGaS_2$ and $RbGaS_2$ compounds.

The crystallographic classification of the $A^I B^{III} C_2^{VI}$ type of compounds suggests arrangement them into three structural types, such as *ZnS*-, *NaCl*-, and *TISe*, which enables the discovery of other $A^I B^{III} C_2^{VI}$ compounds, which have not yet been investigated.

References

[1] Boyd, G., H. Kasper, and J. McFee, Linear and nonlinear optical properties of LiInS2. Journal of Applied Physics, 1973. 44(6): p. 2809-2812.

[2] Negran F. J, Kaspe H. M. and A. M. Glass, "Pyroelectric and electrooptic effects in $LiInS_2$ and $LiInSe_2$" Mater. Res. Bull, (1973) 8, 743.

[3] Kovach, S., et al., Preparation and basic physico-chemical properties of alkali metal indates and thioindates. Izv. Akad. Nauk SSSR, Neorg. Mater, 1978. 14(12): p. 2172-2176.

[4] Kish, Z.Z., formation, crystalographic classification and properties of compounds in ai-biii-cvi systems.

[5] Krebs, B., Thio-und Selenoverbindungen von Haupt gruppenelementen-neue anorganische Oligomere und Polymere. Angewandte Chemie, 1983. 95(2): p. 113-134.

[6] Delgado, G., et al., Growth and crystal structure of the layered compound TlGaSe2. Crystal Research and Technology: Journal of Experimental and Industrial Crystallography, 2007. 42(7): p. 663-666.

[7] Kumari, A. and K. Vidyasagar, Rubidium thiogallate. Acta Crystallographica Section E: Structure Reports Online, 2005. 61(9): p. i193-i195

[8] Friedrich, D., et al., Polymorphism of CsGaS 2–structural characterization of a new two-dimensional polymorph and study of the phase-transition kinetics. Inorganic Chemistry Frontiers, 2017. 4(2): p. 393-400.

Chapter II

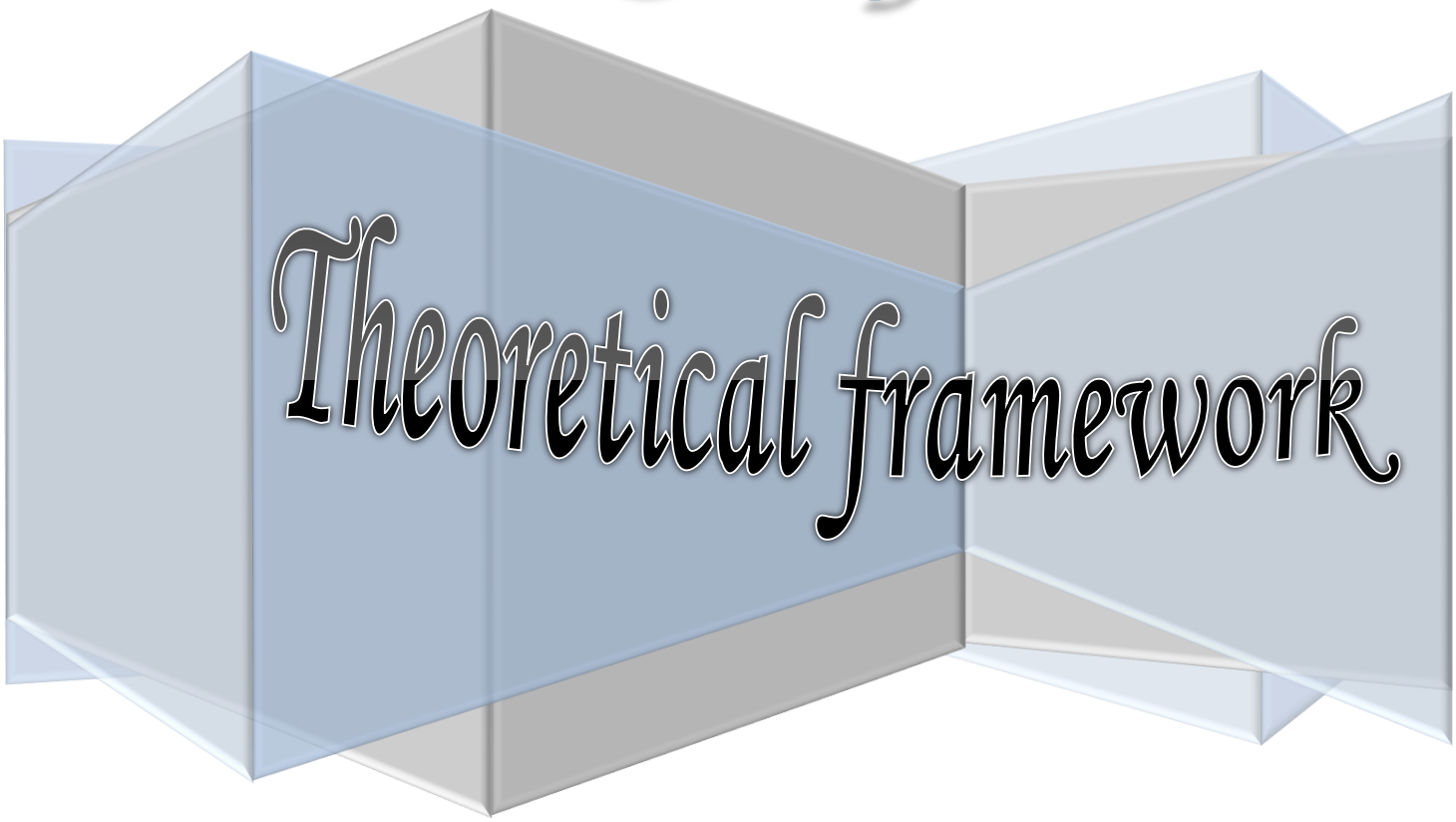

II.1 Introduction

In Schrödinger theory [1], the correlations between electrons are incorporated in the structure of the stationary state wave function Ψ of the system. These correlations arise due to the Pauli exclusion principle and Coulomb repulsion, the former being accounted by the requirement that the wave function must be anti-symmetric in an interchange of the coordinates (including spin) of any two electrons. However, due to the two-particle electron-interaction operator in the Hamiltonian, the analytical dependence of the wave function on the electronic coordinate's representative of Coulomb correlations is unknown. Properties of the system are determined as expectation values of operators representing the observables of interest, taken with respect to the wave function. Thus the energy is the expectation value of the Hamiltonian. Now according to the first theorem of modern density-functional theory [2], due to Hohenberg and Kohn [3], the ground-state wave function Ψ is a functional of the exact ground-state electronic density ρ (r).

Density functional methods has emerged in the early days of quantum mechanics. However, the foundations of the modern density functional theory (DFT) were established in the mid *1960* with the classical papers by Hohenberg and Kohn (*1964*) and Kohn and Sham (*1965*) [4].

II.2 The Schrödinger equation

Schrödinger proved that a normal but somewhat mysterious quantization rule is naturally provided by assuming the finiteness and definiteness of a spatial function (Schrödinger *1926*) [1].

If we restrict our discussion to stationary electronic states, then we need to consider the time-independent version of the Schrödinger equation.

$$\left[\frac{\vec{p}^2}{2m_e} + V(\vec{r})\right]\Psi(\vec{r}) = E(\vec{r})\Psi(\vec{r}) \qquad \textbf{(II.1)}$$

Where m_e is the electron mass, and the quantum-mechanical momentum operator is given by:

$$\vec{p} = -i\hbar\vec{\nabla}; \qquad \vec{\nabla} = \vec{u}_x\frac{\partial}{\partial x} + \vec{u}_y\frac{\partial}{\partial y} + \vec{u}_z\frac{\partial}{\partial z} \qquad \textbf{(II.2)}$$

For a molecular system of N-electrons and N nuclei, the Schrödinger equation is **[6]:**

$$\hat{H}\Psi(\vec{r_i},\vec{R_j}) = E\Psi(\vec{r_i},\vec{R_j}) \qquad \textbf{(II.3)}$$

- where the Hamiltonian operator H is:

$$\hat{H} = \hat{T}_e + T_N + V_{ee} + V_{NN} + V_{Ne} \qquad \textbf{(II.4)}$$

Atomic units (Ua) [5]: In the following we will try to simplify the writing of the equations in order to get a feeling of what a solution would look like. Before doing so it is convenient to do some housekeeping with the units of measurement.

$\hbar = 1{,}05457163.10^{-34}$ J.s,

$m_e = 9{,}10938291.10^{-31}$Kg,

$m_p = 1{,}67262164.10^{-27}$ Kg,

$e = 1{,}60217649.10^{-19}$C,

$\varepsilon_0 = 8{,}85418782.10^{-12}$F.m^{-1}.

After using this units we can write Schrödinger equation in the form:

$$\hat{H}\Psi = \frac{-\hbar^2}{2}\sum_{i=1}^{n}\frac{\vec{\nabla}^2_{\vec{R}_i}}{M_i} - \frac{-\hbar^2}{2}\sum_{i=1}^{n}\frac{\vec{\nabla}^2_{\vec{r}_i}}{m_e} - \frac{e^2}{4\pi\varepsilon_0}\sum_{i,j}^{n}\frac{Z_i}{|\vec{R}_i - \vec{r}_j|} + \frac{e^2}{8\pi\varepsilon_0}\sum_{i\neq j}^{n}\frac{1}{|\vec{r}_i - \vec{r}_j|} + \frac{e^2}{8\pi\varepsilon_0}\sum_{i\neq j}^{n}\frac{Z_i Z_j}{|\vec{R}_i - \vec{R}_j|} \qquad \textbf{(II. 5)}$$

- ✓ E is the total energy.
- ✓ **the** wave function Ψ is : $\Psi = \Psi(\vec{r}_1,\vec{r}_2,\vec{r}_3 \dots\dots\dots \vec{r}_n,\overrightarrow{R_1},\overrightarrow{R_2},\dots\dots\dots,\overrightarrow{R_N})$
- ✓ $\mathbf{r_i}$ the position vector of the electron i.
- ✓ $\mathbf{R_N}$ the position vector of the nucleus (ion) N.
- ✓ $\boldsymbol{m}_e$ the mass of the electron ***i*** and ***e*** its charge.
- ✓ $\boldsymbol{M}_j$ the mass of the nucleus j.
- ✓ $\boldsymbol{Z_{k,l}}$ the atomic number of the nuclei k and l.
- ✓ $\boldsymbol{r_{i,j}}$ and $\boldsymbol{R_{K,l}}$ electronic coordinates (i and j) and nuclei (k and l) respectively.

The mass of the nucleus at $\vec{R_i}$ is M_i, the electrons have mass m_e and are at $\vec{r_i}$. The first term is the kinetic energy operator for the nuclei, the second for the electrons.

The last three terms describe the Coulomb interaction between electrons and nuclei, between electrons and other electrons**,** and between nuclei and other nuclei. It is out of question to solve this problem exactly. In order to find acceptable approximate eigenstates**,** we will need to make approximations, we begin with the first approximation introduced by Born-Oppenheimer [6].

II.3 The Born-Oppenheimer Approximation

The Born-Oppenheimer approximation is to decouple the movement electrons from that of the nuclei. Indeed, the ratio between the mass of the electron and the mass of any atomic nucleus is very weak. So the electrons move so much faster than atomic nuclei. In this approximation, the electrons are always in their fundamental state, whatever the position of the atomic nuclei. The problem therefore goes from a system of N_e+ N_n interacting particles to a system of N_e interacting electrons in an external potential generated by the nuclei. The positions of atomic nuclei are just parameters in solving the problem. The interaction term between the nuclei only intervenes in the calculation of the total energy of the system**,** but not in the calculation of the electronic wave functions.

The Hamiltonian reduced to its only electronic components is therefore written as:

$$\hat{H}_e = \hat{T}_e + \hat{V}_{ee} + \hat{V}_{Ne} \qquad \textbf{(II.6)}$$

We can than write a Schrödinger equation on electrons:

$$\hat{H}_e \Psi_e = E_e \Psi_e \qquad \textbf{(II.7)}$$

The wave function of system as a product of two wave functions:

$$\Psi\,[\{\vec{R}_i\},\{\vec{r}_i\}] = \Psi_e\,[\{\vec{R}_i\},\{\vec{r}_i\}]\times\varphi_n[\{\vec{R}_I\}] \qquad \textbf{(II.8)}$$

This approximation reduces considerably the complexity of the many body-quantum problem of interacting particles, but the obtained electronic Schrödinger equation is still very hard to solve due to the mutual electronic interactions, so physicists need more approximations to solve the problem.

II.4 Hartree and Hartree-Fock approximation

Suppose we would like to approximate the wave function of n electrons**.** Let us assume for the moment that the electrons have no effect on each other. If this is true, the Hamiltonian for the electrons may be written as where h_i describes the kinetic and potential energy of electron i.

$$\hat{H} = \sum_{i=0}^{n} h_i \qquad \textbf{(II.9)}$$

If we write down the Schrodinger equation for just one electron based on this Hamiltonian, the solutions would satisfy the eigen functions defined by this equation which are called spin orbitals [7].

$$\hat{H}\Psi(\vec{r}_i) = \varepsilon_i \Psi_i(\vec{r}_i) \qquad \textbf{(II.10)}$$

And

$$\hat{H}_H = -\frac{1}{2}\nabla_i^2 + V_{ext}(\vec{r},\vec{R}) + V_H(\vec{r}) \qquad \textbf{(II.11)}$$

Where:

- $V_{ext}(\vec{r},\vec{R})$: the potential due to the electron-nuclei interactions.
- $V_H(\overrightarrow{r})$:the potential of Hartree associated with Coulomb interaction with other electrons.

Where the total Hamiltonian is simply a sum of one-electron operators, hi, it follows that the eigen functions of Hartree is the products of the one-electron spin orbitals:

$$\Psi[\{\vec{r}_e\},\{\vec{R}_i\}] = \Psi_1(\vec{r}_1).\Psi_2(\vec{r}_2).....\Psi_{Ne}(\vec{r}_{Ne}) \qquad \textbf{(II.12)}$$

The energy of this wave function is the sum of the spin orbital energies:

$$\varepsilon_i = \varepsilon_{1+}\ \varepsilon_2 ..... \varepsilon_{Ne}.$$

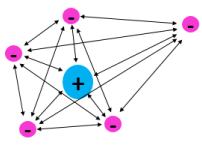

Figure II .1: *Many-electron systems. All electron- electron repulsion is included explicitly.*

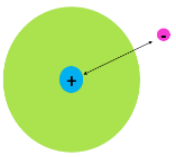

Figure II .2: *one-electron systems with remaining electrons represented by an average charge density.*

The Hartree product does not satisfy all the important criteria for wave functions**.** Because electrons are fermions, the wave function must change sign if two electrons change places with each other. This is known as the anti-symmetry principle**.** Exchanging two electrons does not change the sign of the Hartree product**,** which is a serious drawback.

Hartree-Fock suggested that the wave function is a slater-determinant:

$$\Psi_e=\Psi_{DS}=\frac{1}{\sqrt{N!}}\begin{vmatrix}\Psi_1(\vec{r}_1) & \cdots & \Psi_N(\vec{r}_1)\\ \vdots & \ddots & \vdots\\ \Psi_1(\vec{r}_N) & \cdots & \Psi_N(\vec{r}_N)\end{vmatrix} \qquad \textbf{(II.13)}$$

- $\frac{1}{\sqrt{N!}}$**:** Normalization factor.

We can obtain a better approximation to the wave function by using a Slater determinant. In a Slater determinant, the N electron wave function is formed by combining one-electron wave functions in a way that satisfies the anti-symmetry principle**.** This means that the Slater determinant satisfies the conditions of the Pauli Exclusion Principle.

$$\left(-\frac{1}{2}\nabla_i^2+V_{ext}\left(\vec{r}\ ,\vec{R}\ \right)+\sum_{i\neq j=1}^{n}\int\frac{\left|\varphi_j(\vec{r})\right|^2}{\left|\vec{r}-\vec{r}\right|}d\vec{r}\right)\varphi_i(\vec{r})-$$

$$+\sum_{i\neq j=1}^{n}\int\frac{\varphi_j(\vec{r})\varphi_j^*(\vec{r})}{\left|\vec{r}-\vec{r}\right|}d\vec{r}\varphi_i(\vec{r})=\varepsilon_i\,\varphi_i(\vec{r}) \qquad \textbf{(II. 14)}$$

- ✓ $-\frac{1}{2}\nabla_i^2$: The kinetic energy of the electron i.
- ✓ $V_{ext}\left(\vec{r}\ ,\vec{R}\ \right)$: The energy of attraction between nuclei and electrons.
- ✓ $\sum_{i\neq j=1}^{n}\int\frac{\left|\varphi_j(\vec{r})\right|^2}{\left|\vec{r}-\vec{r}\right|}d\vec{r}$: The integral of Coulomb noted (the potential of Hartree).
- ✓ $\sum_{i\neq j=1}^{n}\int\frac{\varphi_j(\vec{r})\varphi_j^*(\vec{r})}{\left|\vec{r}-\vec{r}\right|}d\vec{r}$: The exchange integral.

In a Hartree–Fock (HF) calculation, we fix the positions of the atomic nuclei and aim to determine the wave function of N-interacting electrons.

II.5 Density functional theory (DFT)

Density functional theory (DFT) is currently one of the most successful and popular quantum mechanical approaches to describe matter. Its applicability ranges from atoms to molecules and solids, including quantum and classical fluids. Indeed, DFT is routinely used nowadays for calculating a great variety of properties in chemistry (e.g. molecular structures, reaction paths, etc.) and in physics (e.g. band structures of solids) [1].

The basic principle of the density functional theory emerged in the nineteen-twenties with the work on the uniform electron gas of Thomas and Fermi [8, 9], who came up with the idea that the energy of a system is given completely in terms of its electron density. However, only in *1964*, with the publication of the Hohenberg and Kohn (H-K) theorems [10], and in *1965*, with the derivation of the set of monoelectronic equations with which one can obtain the ground state density (Kohn-Sham equations) [11].

II.5.1 Thomas –Fermi approximation

The idea of replacing the wave function with the charge density was proposed in *1927* [8], resulting in the so-called Thomas–Fermi approach to electronic structure. Dirac improved the theory by including a term describing the exchange energy [11].

The total energy of the system is written as:

$$E_{TF} = C_1 \int \rho(\vec{r})^{5/3} d\vec{r} + \int V_{ext}(\vec{r})\rho(\vec{r})\, d\vec{r} + C_2 \int \rho(\vec{r})^{4/3}\, d\vec{r} + \\ + \frac{1}{2}\int \frac{\rho(\vec{r})\rho(\vec{\dot{r}})}{|\vec{r} - \vec{\dot{r}}|} d\vec{r} d\vec{\dot{r}} \qquad (\mathbf{II.15})$$

With $C_1 = (3/10)(3\pi^2)^{2/3}$ and $C_2 = -(3/4)(3/\pi)^{1/3}$. The first term describes the kinetic energy, then follows the electron–nuclei interaction, the exchange and finally the Hartree term. In the expression above, the kinetic energy and correlation terms of the many-electron system are calculated assuming a homogeneous electron gas (HEG). The HEG is of fundamental importance in DFT, and thus we repeat its definition here

and also the definition of the often used parameters. The density ρ of the homogeneous electron gas is:

$$\rho = \frac{n}{\Omega} \qquad (\mathbf{II.16})$$

Where n is the total number of electrons in the volume Ω.

The Thomas–Fermi theory failed to produce any quantitatively impressive results**,** but the basic idea of using the electron charge density as the basic variable instead of the wave function turned out to be most fruitful.

II.5.2 The Hohenberg-Kohn (HK) theorems

In *1964*, the concept of the Thomas–Fermi method was revived by the so-called Hohenberg–Kohn theorem [12].This theorem consists of the following two major theorems for no degenerate ground electronic states:

- The electron density determines external potentials, which correspond to the nuclear–electron interaction potentials in the absence of an electromagnetic field.
- The energy variational principle is always established for any electron density.

Since these theorems were also proven mathematically, establishing the validity of the concept [13], they can be interpreted as the basic theorems of a quantum theory based on electron density.

The Hamiltonian $\hat{H}_N$of this system of electrons in atomic units ($e = \hbar = m = 1$) is the sum of its kinetic $\hat{T}$, electron-interaction potential energy $\hat{U}$, and external potential energy $\hat{V}$operator:

$$\hat{H}_n = \hat{T} + \hat{U} + \hat{V} \qquad (\mathbf{II.17})$$

Where

$$\hat{T} = -\frac{1}{2}\sum_{i=1}^{n}\nabla_i^2;\ \hat{U} = \frac{1}{2}\sum_{i\neq j}^{n}\frac{1}{|\vec{r_i}-\vec{r_j}|};\ \hat{V} = \sum_{i=1}^{n} v(\vec{r_i})$$

With $\vec{r}$=$\vec{r}_1$……..$\vec{r}_n$.

The corresponding Schrödinger equation is:

$$\hat{H}_N\Psi_n(\{\vec{r_i}\},\{\vec{R_j}\}) = E_n\Psi_n(\{\vec{r_i}\},\{\vec{R_j}\}) \qquad (\mathbf{II.18})$$

The energies E_n are the expectation:

$$E_n = \langle \Psi_n | \hat{H}_N | \Psi_n \rangle, \qquad \textbf{(II. 19)}$$

And the density ρ(r) the expectation:

$$\rho_n(\vec{r}) = \langle \Psi_n | \hat{\rho}(\vec{r}) | \Psi_n \rangle \qquad \textbf{(II. 20)}$$

The First Hohenberg-Kohn Theorem (Theorem 1):

The no degenerate ground state density $\rho(\vec{r})$ determines the external field $\varepsilon(\vec{r})$ or equivalently the external potential $v(\vec{r})$ to within a trivial additive constant.

Consider the case of no degenerate ground states**.** With the kinetic $\hat{T}$ and electron interaction Û potential energy operators known**,** different external fields with potential energy operators $\hat{V} = \sum_i v(\vec{r_i})$ lead via solution of the time-independent Schrödinger equation to different ground state wave functions ψ. This defines the map C between the potential energies and $v(\vec{r})$ the wave functions ψ (see **Figure. II.3**)**.** These different ground state wave functions then lead via (II. 20) to different ground state densities $\rho(\vec{r})$. This establishes the map D between wave functions and densities. The combination (CD) of the maps C and D then maps each potential energy $v(\vec{r})$ to a ground state density $\rho(\vec{r})$.

To show the invertibility C^{-1} of map C**,** what needs be proved is that two different external potential energy operators $\hat{V}$ and $\hat{V}'$ that differ by more than a constant such that $\hat{V} \neq \hat{V}'$+constant**,** must lead to different ground state wave functions ψ and ψ ′.

To show the invertibility D^{-1} of map D**,** one must employ the conclusions of Map C**,** i.e. that there exists only one ψ for each V(r).

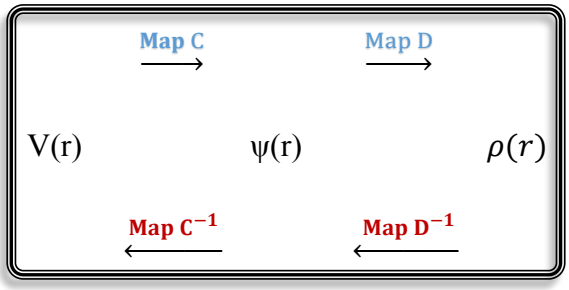

Figure II .3: *Maps relating the correspondence between external potential energies, ground state wave functions, and ground state densities.*

The Second Hohenberg-Kohn Theorem (Theorem 2):

The no degenerate ground state density can $\rho(\vec{r})$ be determined from the ground state energy functional E $[\rho]$ via the variational principle by variation only of the density.

The ground state energy E which is a functional of the density is:

$$E \equiv E[\rho] = \langle \psi[\rho] | \hat{H} | \psi[\rho] \rangle \qquad (\mathbf{II.21})$$

Consider atrial v–representable ground state density $\tilde{\rho}(\vec{r})$. From Theorem 1 this density determines the corresponding external potential energy $\tilde{v}(\vec{r})$, and via the resulting Hamiltonian the trial wave function $\tilde{\Psi}[\tilde{\rho}]$. Equivalently, $\tilde{\Psi}[\tilde{\rho}]$ is determined from the inverse map D^{-1} from the variational principle for the energy it follows that:

$$\tilde{E} = E[\tilde{\rho}] \langle \tilde{\Psi}[\tilde{\rho}] | \hat{H} | \tilde{\Psi}[\tilde{\rho}] \rangle > \mathrm{E} \text{ for } \tilde{\rho}(\vec{r}) \neq \rho(\vec{r})$$

$$= \mathrm{E} \text{ for } \tilde{\rho}(\vec{r}) = \rho(\vec{r}) \qquad (\mathbf{II.22})$$

II.5.3 The Kohn-Sham equation

The Hohenberg-Kohn theorem tells us that the total energy of many electrons in their ground state is a functional of the electron density. However, this theorem does not say anything about how to construct such functional**.** While the exact form of this functional is still unknown, since the original work by Hohenberg and Kohn a number of very useful approximations have been developed.

The Kohn–Sham method is a variational approach using the electron–electron interaction potential of the density functional to give the lowest energy and the corresponding molecular orbitals and orbital energies. From a practical viewpoint**,** the most significant characteristic of this method is the use of the independent-electron approximation of kinetic energy, similarly to the Hartree–Fock method, instead of the kinetic energy functional in the Thomas–Fermi method [11].

The Hohenberg Kohn variational principle can be recast in the form of exact single particle self-consistent equations**,** similar to the Hartree equations:

$$\left(-\frac{\hbar^2}{2m} \nabla^2 + v_{\text{eff}}(\vec{r}) \right) \Psi_j(\vec{r}) = \varepsilon_j \Psi_j(\vec{r}), \qquad (\mathbf{II.23})$$

$$\rho(\vec{r}) = \sum_{j=1}^{N} |\Psi_j(\vec{r})|^2 \qquad \textbf{(II. 24)}$$

And $$v_{\text{eff}} = v(\vec{r}) + \int \frac{n(\vec{r})}{|\vec{r}-\vec{r}|} d\vec{r} + v_{xc}(\vec{r})$$

Where $v_{xc}(\vec{r})$ is the local exchange-correlation potential, defined as:

$$v_{xc}(\vec{r}) = \frac{\delta E_{xc}[\rho(\vec{r})]}{\delta \rho(\vec{r})} \qquad \textbf{(II. 25)}$$

$$\mathrm{E}_{xc}[\rho(\vec{r})] = F[\rho(\vec{r})] - \frac{1}{2}\int \frac{\rho(\vec{r})\rho(\vec{r})}{|\vec{r}-\vec{r}|} d\vec{r} - T_S[\rho(\vec{r})],$$

Where $T_S[\rho(\vec{r})]$ is the kinetic energy of non-interacting electrons with ground state density $\rho(\vec{r})$.

In the LDA, $v_{xc}(\vec{r})$ becomes simply

$$v_{xc}^{LDA}(\vec{r}) = \frac{d}{d\rho}(\rho\varepsilon_{xc}(\rho))|_{\rho=\rho(r)} \qquad \textbf{(II. 26)}$$

Solution of the equations (II. 23) yields $\rho(r)$ and allows calculation of the ground state energy:

$$E = \sum_{j=1}^{N} \varepsilon_j - \frac{1}{2}\int \frac{\rho(\vec{r})\rho(\vec{r})}{|\vec{r}-\vec{r}|} d\vec{r} - \int v_{xc}(\vec{r})\rho(\vec{r})d\vec{r} + E_{xc}[\rho(\vec{r})]. \qquad \textbf{(II. 27)}$$

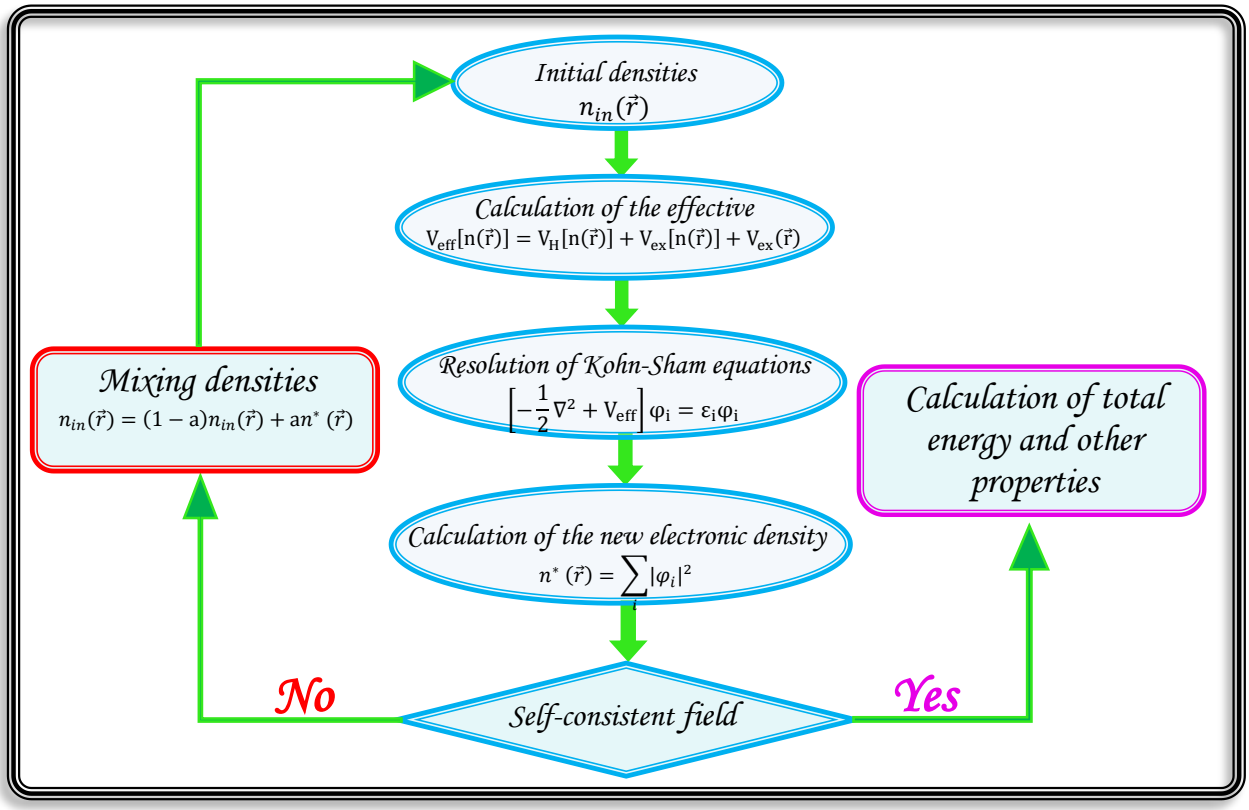

Figure II .4: *Flowchart of DFT self-consistent cycle calculation.*

As illustrated in **Figure II.4**, the self-consistent resolution of the KH equations starts with the construction of a guest density. Than the effective potential is calculated and the resulting mono-electronic KH equations are solved. With the obtained engine states, also called KH pseudo-orbitals, a new density is constructed and the self-consistency of the new density and the corresponding energy is are tested. If the self-consistency is achieved than the ground state properties can be calculated, otherwise, a new density is constructed by mixing the last two densities, and the SCF cycle is looped.

II.5.4 The exchange and correlation functional

II.5.4.1 Local density approximation (LDA)

Since the introduction of the Kohn-Sham theory a great deal of effort has been devoted to constructing accurate exchange and correlation functionals, $E_{xc}[\rho]$ in order to solve the Kohn-Sham equations. As a result several approximate functionals are available today. Here we describe the simplest functional, which goes under the name of the local density approximation (LDA) to density functional theory **[14, 15]**.

To understand the concept of an LDA recall first how the no interacting kinetic energy $T_s[\rho]$ is treated in the Thomas-Fermi approximation:

$$t_s^{hom}(\rho) = \frac{3\hbar^2}{10m}(3\pi^2)^{2/3}\rho(\vec{r})^{5/3} \qquad (\mathbf{II.28})$$

Where $\rho = const$. In an inhomogeneous system, with $\rho = \rho(\vec{r})$, one approximates locally:

$$t_s(\vec{r}) \approx t_s^{hom}\big(\rho(\vec{r})\big) = \frac{3\hbar^2}{10m}(3\pi^2)^{2/3^2}\rho(\vec{r})^{5/3} \qquad (\mathbf{II.29})$$

And obtains the full kinetic energy by integration over all space:

$$T_S^{LDA}[\rho] = \int t_s^{hom}\big(\rho(\vec{r})\big)d\vec{r} = \frac{3\hbar^2}{10m}(3\pi^2)^{2/3}\int \rho(\vec{r})^{5/3}d\vec{r} \qquad (\mathbf{II.30})$$

For the kinetic energy the approximation LDA $T_S[\rho] \approx T_S^{LDA}[\rho]$ is much inferior to the exact treatment of T_S in terms of orbitals, offered by the Kohn-Sham equations**,** but the LDA concept turned out to be highly useful for another component of the total energy, the exchange-correlation energy$E_{xc}[\rho]$.

For the exchange energy $E_{xc}[\rho]$ the procedure is very simple, since the per volume exchange energy of the homogeneous electron liquid is known exactly [16, 17]:

$$e_x^{hom}(\rho) = -\frac{3q^2}{4}\left(\frac{3}{\pi}\right)^{1/3}\rho(\vec{r})^{4/3} \qquad (\mathbf{II.31})$$

So that $$E_X^{LDA}[\rho] = -\frac{3q^2}{4}\left(\frac{3}{\pi}\right)^{1/3}\int \rho(\vec{r})^{4/3}d\vec{r} \qquad (\mathbf{II.32})$$

II.5.4.2 Generalized Gradient Approximation (GGA)

In a molecular system, the electron density is typically rather far from spatially uniform**,** so there is good reason to believe that the LDA approach will have limitations. One obvious way to improve the correlation functional is to make it depend not only on the local value of the density, but on the extent to which the density is locally changing**,** i.e., the gradient of the density. Such an approach was initially referred to as 'non-local' DFT because the Taylor-expansion-like formalism implies reliance on values of the density at more than a single position. However, mathematically speaking, the first derivative of a function at a single position is a local property**,** so the more common term in modern nomenclature for functional that depend on both the density and the gradient of the density is 'gradient corrected'. Including a gradient correction defines the 'generalized gradient approximation' (GGA).

Most gradient corrected functional are constructed with the correction being a term added to the LDA functional, i.e.

$$E_{xc}^{GGA}\left[\rho(\vec{r}),\vec{\nabla}\rho(\vec{r})\right] = \int \rho(\vec{r})\varepsilon_{xc}^{GGA}\left[\rho(\vec{r}),\nabla\rho(\vec{r})\right]d\vec{r} \qquad (\mathbf{II.33})$$

Alternative GGA exchange functional have been developed based on rational function expansions of the reduced gradient**.** These functional, which contain no empirically optimized parameters, include *B86*, *PW*, *WC*, *PBE*.

II.5.4.3 Hybrid Functional HS

Hybrid functional mix the Hartree–Fock exchange integral with GGA exchange functional at a constant ratio, based on the concept of the adiabatic connection, which makes the Kohn–Sham energies of the independent electron model link to those of the fully interacting electron one. That is**,** hybrid functional are constructed by connecting exchange functional, which are assumed as the exchange energies of the independent

electron systems, to the Hartree–Fock exchange integral, which are taken as the exchange energies for the fully interacting systems,

$$E_{XC} + 9\int_0^1 d\lambda E_{XC}^{\lambda} \cong E_X^{GGA} + \lambda(E_{xc}^{HF} - E_{xc}^{GGA}) \qquad (\mathbf{II.34})$$

Where λ is termed the coupling strength parameter.

Many new hybrid functionals have been recently developed**.** In these models, the exchange-correlation energy functional makes both Hartree-Fock and other formalism of the DFT (LDA or GGA), hence their name of hybrid functionals. Currently, the most common hybrid functionals are *PBE0*, *HSE03*, *HSE06* and *B3LYP* **[18]**.The use of such functionals makes it possible to accurate results which compare well with their experimental counterpart , such as equilibrium geometries**,** or band gap energies.

In general, hybrid functionals are particularly effective for the description of molecules, insulating materials, semiconductors and transition metal oxides. Their major disadvantage is that such calculations are generally greedy in computing resources than for conventional functional, because of the incorporation of the Hartree-Fock terms.

II.6 Calculation methods

II.6.1 Pseudo potential method

The fundamental idea of pseudo potentials is to replace the real potential, arising from the nuclear charge and the core electrons, with an effective potential, within a core region of radius R_c , as illustrated schematically in **Figure II.5**, some requirements are then placed on this effective potential. It must be such that the valence orbital eigenvalues are the same as those in an all-electron calculation on the atom. It must also preserve the continuity of the wave functions and their first derivatives across the core boundary. Finally, charge density in the core region should be same as an all-electron density, that is, the pseudo potential must be norm-conserving. A pseudo potential that satisfies these requirements will have the same scattering properties, at energies corresponding to valence eigenvalues, as the ionic core it replaces.

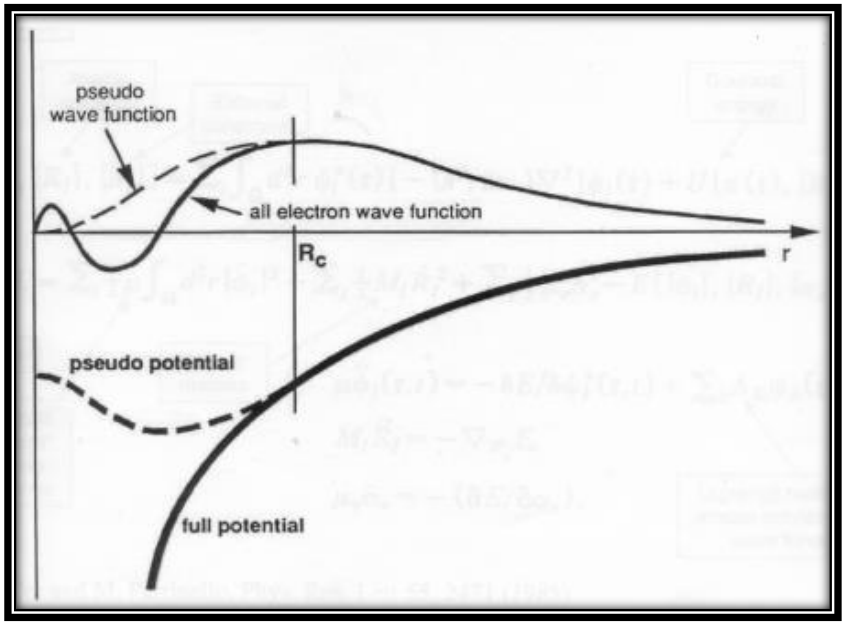

Figure II .5: *Schematic illustration of all-electron (solid lines) and pseudo electron (dashed lines) potentials and their corresponding wave functions. The radius at which all-electron and pseudo electron values match is designated* R_c [19].

II.6.2 Plans waves

The plane-wave pseudo potential (PW-PP) method begins by representing the system by a 3-dimensional periodic super cell. This allows Bloch's theorem to simplify the task of solving the Kohn-Sham equation. This is because Bloch's theorem which is based upon the periodicity of the system, reduces the infinite number of one-electron wave functions in the real system to only the number of electrons in the chosen super cell.

$$\Psi_{n,k}(\vec{r}) = u_{n,k}(\vec{r})\exp(i\vec{k}.\vec{r}) \qquad \textbf{(II. 34)}$$

The function $u(\vec{r})$ has the periodicity of the super-cell**.** It can be of any suitable mathematical form, and usually one chooses a series expansion in terms of a set of basis functions**.** In PW-PP approach, plane waves are used for this expansion, so that each single-electron wave function$\Psi_{n,k}$is written as:

$$\Psi_{n,k}(\vec{r}) = \sum_{G} C_{n,k}(\vec{G})\exp\left(i(\vec{k}+\vec{G}).\vec{r}\right) \qquad \textbf{(II. 35)}$$

They $C_{n,k}(\vec{r})$ are the expansion coefficients. The wave vectors $\vec{G}$ are such that the plane waves are commensurate with the super-cell. Both the number of G-vectors in the sum and the number of k's considered in principle to be infinite.

II.7 Practical aspects of DFT Calculations

II.7.1 Periodic Systems and Bloch theorem

The Bloch theorem is a consequence of the translational invariance of the Hamiltonian for an infinite periodic crystalline solid. The Hamiltonian commutes with the translation operator P_R associated with a lattice vector $\overrightarrow{R}$,

$$[H, P_R] = 0 \qquad (\mathbf{II.37})$$

Consequently, any eigenstates of H is also an eigenstates of P_R. One first shows that the eigenvalue equation for P_R can be written in the form

$$P_R \phi_K(\vec{r}) = e^{i\vec{K}\vec{R}} \phi_K(\vec{r}) \,, \qquad (\mathbf{II.38})$$

So that the wave vector labels the eigenvectors and eigenvalues of H, i.e.

$$\hat{H}\phi_K(r) = E_K \phi_K(r) \qquad (\mathbf{II.39})$$

Finally, one shows that Eq (II. 35) requires that $\phi_K(\vec{r})$ must have the form $\phi_K(\vec{r}) = e^{i\vec{K}\vec{r}} u_k(\vec{r})$, where $u_k(\vec{r})$ has the full crystal periodicity i.e. $P_R u_k(\vec{r}) = u_k(\vec{r})$. One normally introduces Born-Von-Karman (BVK) boundary conditions, large periodic cells of volume L^3 in which the Bloch functions $\phi_K(\vec{r})$ are normalized to unity. It is this identical normalization in every BVK cell that imposes the usual requirement that k is real.

The Schrödinger equation and the generalized Bloch theorem can be combined into a single "transfer-matrix equation" which allows evanescent solutions. This result has been derived in previous works for various forms of the Hamiltonian, namely, for pseudo potentials [20].

II.7.2 Sampling of the Brillion Zone (BZ)

In the previous section we introduced $\vec{K} = k_1\vec{b}_1 + k_2\vec{b}_2 + k_3\vec{b}_3$ as a convenient index to label the wave functions. Here we will show that this index actually has physical meaning. Consider that the crystal is composed of N_j unit cells in the direction of vector $\vec{a}_j$ $(j = 1,2,3)$, where we think of the values of as macroscopically large. $N = N_1N_2N_3$ Is equal to the total number of unit cells in the crystal (of order

Avogadro's number, 6.023×10^{23}).We need to specify the proper boundary conditions for the single-particle states within this crystal. Consistent with the idea that we are dealing with an infinite solid**,** we can choose periodic boundary conditions, also known as the Born–von Karman boundary conditions,

$$\Psi_k(\vec{r}) = \Psi_k(\vec{r} + N_j \vec{a}_j) \qquad (\mathbf{II.40})$$

The volume in reciprocal space is known as the first Brillouin Zone (BZ in the following). By convention**,** we choose the first BZ to correspond to the following N_j consecutive values of the index n_j:

$$n_j = -\frac{N_j}{2}, \ldots, 0, \frac{N_J}{2} - 1 \qquad (j = 1,2,3,) \qquad (\mathbf{II.41})$$

Where we assume $N_j$to be an even integer (since we are interested in the limit $N_j \to \infty$ this assumption does not impose any significant restrictions).

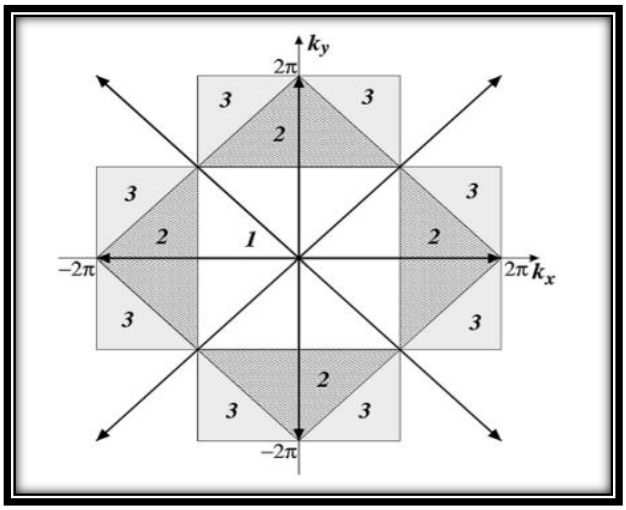

FigureII .6: *Illustration of the construction of Brillouin Zones in a two-dimensional crystal.*

II.8 Calculation Code: CASTEP

In this work, the plane wave pseudo potential (PP-WP) calculations for the solution of the Kohn Sham equation of Density Functional Theory (DFT) were performed using CASTEP (Cambridge Serial Total Energy Package) [21].with the generalized gradient approximation for the exchange correlation energy functional. CASTEP is a pseudo potential total-energy code which employs special point integration over the Brillouin zone and a plane wave basis for the expansion of the wave functions. We used the PBE form of the GGA, which was designed to be more robust and accurate than the original GGA formulation. CASTEP, performs a variational

solution to the Kohn-Sham equations by using a density mixing scheme to minimize the total energy and also conjugate gradients as well as the BFGS algorithm to relax the ions under the influence of the Hellmann-Feynman forces. Electronic band structure calculations and optical properties can be predicted with sufficient accuracy to get new insights on the yet not explored fundamental ground state properties of virtually any material.

II.9 Conclusion

In this chapter; we are now studying the Schrödinger equation starting with approximation B-O described as adiabatic because it consists of separating the electronic problem from that of the vibrations of the network whereas with Hartree the treatment consists of reducing the problem of n body to single particle which results in Slater's approximation of the exchange term assuming that it has a local character unlike the AHF.

The energy of an electron system interacting in a potential depends on the distribution of density of these electrons. This idea forms the basis of the Thomas-Fermi method.

Kohn-Sham (KS) formulated the exact energy of the fundamental state of an interacting system into V_{ext} potential dependent solely on electronic density$\rho(r)$. With the LDA approximation the calculated kinetic energies are significantly worse compared to those derived from the Kohn-Sham equations. For the GGA, higher order corrections are difficult to calculate. Moreover, an over view of the CASTEP code is given.

References

[1] Schrödinger, E., An undulatory theory of the mechanics of atoms and molecules. Physical review, 1926. 28(6): p. 1049.

[2] Parr, R.G., W. Yang Density functional theory of atoms and molecules. O xford University Press, 1989. 1: p. 989.

[3] Hohenberg, P. and W. Kohn, Phys Rev 136: B864. Kohn W, Sham LJ (1965) Phys Rev, 1964. 140: p. A1133.

[4] Ernzerhof, M., et al., Density functional theory I: functionals and effective potentials. 1996.

[5] Kiréev, P., La physique des semiconducteurs. 2 e édition, édition Mir. 1975, Moscou

[6] Pisani, C., Quantum-mechanical ab-initio calculation Parr, R.G., W. Yang Density functional theory of atoms and molecules. O xford University Press, 1989. 1: p. 989.of the properties of crystalline materials. Vol. 67. 2012: Springer Science & Business Media.

[7] John Wiley & Sons, Inc, book "density functional theory" A Practical Introduction, Prepared in part with support by the National Energy Technology Laboratory 2009.

[8] Thomas, L. The effect of the orbital velocity of the electrons in heavy atoms on their stopping of α-particles. in Mathematical Proceedings of the Cambridge Philosophical Society. 1927. Cambridge University Press.

[9] Fermi, E., Un metodo statistico per la determinazione di alcune priorieta dell'atome. Rend. Accad. Naz. Lincei, 1927. 6(602-607): p. 32.

[10] Hohenberg, P. and W. Kohn, Inhomogeneous electron gas. Physical review, 1964. 136(3B): p. B864.

[11] Kohn, W. and L.J. Sham, Self-consistent equations including exchange and correlation effects. Physical review, 1965. 140(4A): p. A1133.

[12] Dirac, P.A. Discussion of the infinite distribution of electrons in the theory of the positron. in Mathematical Proceedings of the Cambridge Philosophical Society. 1934. Cambridge University Press.

[13] Kutzelnigg, W.: J. Mol. Struct. Theochem768, 163–173 (2006)

[14] Ceperley, D.M. and B.J. Alder, Ground state of the electron gas by a stochastic method. Physical Review Letters, 1980. 45(7): p. 566.

[15] Perdew, J.P. and A. Zunger, Self-interaction correction to density-functional approximations for many-electron systems. Physical Review B, 1981. 23(10): p. 5048.

[16] Gross, E. and R. Dreizler, Density functional theory: an approach to the quantum many-body problem. 1990, Springer, Berlin.

[17] Calais, J.L., Density-functional theory of atoms and molecules. RG Parr and W. Yang, Oxford University Press, New York, Oxford, 1989. IX+ 333 pp. Price£ 45.00. International Journal of Quantum Chemistry, 1993. 47(1): p. 101-101.

[18] Wahl, R., D. Vogtenhuber, and G. Kresse, SrTiO 3 and BaTiO 3 revisited using the projector augmented wave method: Performance of hybrid and semilocal functionals. Physical Review B, 2008. 78(10): p. 104116.

[19] Calais, J.L., Density-functional theory of atoms and molecules. RG Parr and W. Yang, Oxford University Press, New York, Oxford, 1989. IX+ 333 pp. Price£ 45.00. International Journal of Quantum Chemistry, 1993. 47(1): p. 101-101.

[20] Choi, H.J. and J. Ihm, Ab initio pseudo-potential method for the calculation of conductance in quantum wires. Physical Review B, 1999. 59(3): p. 2267.

[21] Milman, V., et al., Electronic structure, properties, and phase stability of inorganic crystals: A pseudopotential plane-wave study. International Journal of Quantum Chemistry, 2000. 77(5): p. 895-910.

Chapter III

Results and discussion

III.1 Introduction

In this chapter, the obtained results from a theoretical investigation conducted to explore the structural, electronic and optical properties of the monoclinic Structure (*C 2/c*) of the ternary chalcogenides $AGaS_2$ (*A=K, Rb, Cs*) will be presented and discussed.

III.2 Calculation details

DFT Calculations were carried out using the plane wave pseudo-potential method as implemented in the Cambridge Serial Total Energy Package (CASTEP) [1]. The exchange-correlation energy was treated within the generalized gradient approximation with the Perdew-Burke-Ernzerhof (PBE) functional [2]. The core states are treated within the Vanderbilt-type Ultra-soft Pseudo-potential (US-PP) [1]. The *K* ($3s^2 3p^6 4s^1$), *Rb* ($4s^2 4p^6 5s^1$), *Cs* ($5s^2\ 5p^6\ 6s^1$), *Ga* ($3d^{10}\ 4s^2\ 4p^1$), and *S* ($3s^2\ 3p^4$), electronic states were treated as valence electrons. For definite plane wave basis set, Ultra-soft Pseudo-potential (USP) facilitates the calculations with lowest possible cut-off energy with minimum contribution from the core region. It is therefore important to express this energy with the greatest possible precision**.** In order to ensure convergence of the computed structures and energy, the parameters that affect the calculation accuracy were selected after performing careful convergence tests. First, the Cut-off energy (E_{cut}) convergence study has been performed, than convergence with respect to Brillouin zone sampling has been accomplished**,** the results are reported in the next section**.** The self-consistent loop was iterated until the total energy difference of the system between the consecutive iterating steps becomes less than 10^{-6} eV/atom $\left(\frac{E_n - E_{n-1}}{E_n} \leq 10^{-6}\right)$.

III.3 Convergence study

The first step in this work is to determine two essential parameters:

- The Cut-off energy (E_{cut}) to ensure the convergence of the total energy (E_{tot}) and to fix the size of the finite plane wave basis set used in the calculation**.**
- The number of *k*-points *(nkpt)***,** taken into account in integration across the Brillouin zone**,** using the Monkhorst & Pack method [3].

III.3.1 Choice of the size of the plane wave basis set

The calculation codes of DFT use, for the numerical resolution, a decomposition of the Kohn-Sham orbitals on a set of basis functions. The unknowns of the problem becoming the coefficients of the linear combinations of these basis set. In the CASTEP code, they are plane waves, whose mathematical form is well suited to the cases of periodic systems and to the materials containing delocalized electrons such as metals. However, the decomposition of the Kohn-Sham orbitals on a set of basis functions is only accurate when this basis set contains an infinity number of basis functions (which is commonly said to be a complete basis set). In practice, the basis are necessarily truncated, causing errors on total energy and the corresponding ground state density. It is therefore necessary to know the order of magnitude of the calculation error obtained for a given base size. Knowing that the smaller the base, the lower the precision but the faster the calculations are.

In the case of a plane wave basis set, the size of the problem is mainly defined by the energy of the plane wave with the highest frequency (called cut-off energy). The basis size is considered sufficient when the cut-off dependent total energy curve reaches a plateau for a sufficiently low energy. The obtained result are summarised in **Table III.1** and for the sake of clarity, only calculations details for $KGaS_2$ are reported.

Table III.1: *Convergence of total energy as a function of E_{cut} for $AGaS_2$ (A=K, Rb, Cs) with the relative variation of energy (the reference final energy was set to E_{tot} at E_{cut}=600 eV).*

$KGaS_2$		
E_{cut} (eV)	Total Energy (eV)	$\Delta E / E_{tot}$
200	-27095.96042	0.00156
250	-27132.27562	2.2566E-4
300	-27137.70851	2.5464E-5
350	-27138.30173	3.6049E-6
400	-27138.34209	2.1175E-6
450	**-27138.36806**	**1.1607E-6**
500	-27138.38621	4.9207E-7
550	-27138.39284	2.4777E-7
600	-27138.39956	0

For the $AGaS_2$ compounds (A=K, Rb, Cs), the converged total energy is obtained at E_{cut}= 450 eV. Variation of total energy as a function of E_{cut} for these compounds are shown in **Figure III.1**

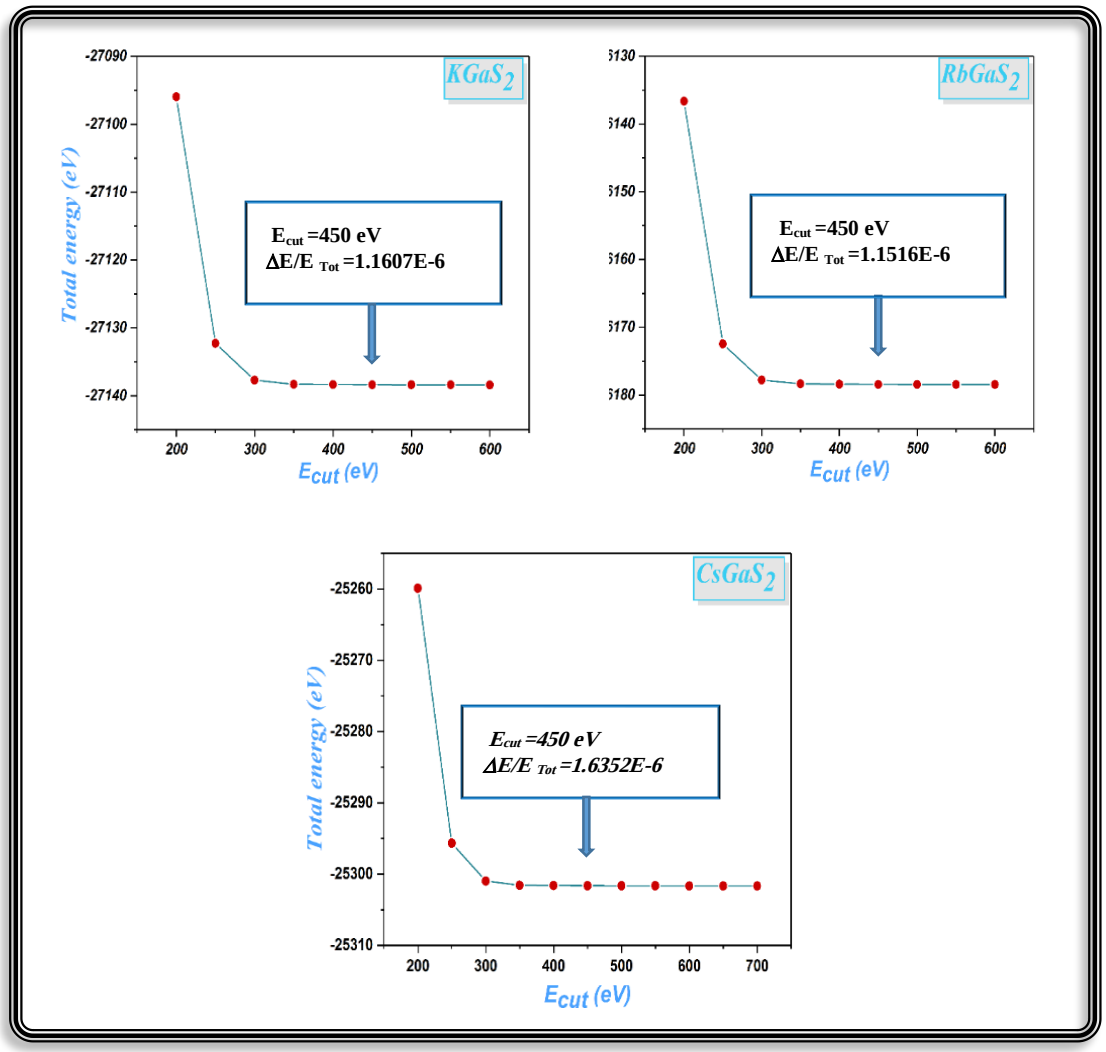

Figure III.1: *Convergence of the total energy as a function of E_{cut} for compounds $AGaS_2$ (A=K, Rb, Cs).*

III.3.2 Brillouin Zone (ZB) Sampling

In a periodic solid, the number of populated Ψ_{nk} mono-electronic orbitals is infinite, with the k-index taking all the values in the BZ. In practice, calculations are necessarily done with a finite number of k-points, which is chosen as low as possible while keeping a representative sampling of the BZ. The most common sampling method is that of Monkhorst & Pack (1976) **[3]**, which makes the sampling as uniform as possible. It is said that the calculation is converged with respect to the number of k-points when the k-point dependant total energy curve reaches becomes stationary.

After setting the value of E_{cut}, we proceed to sampling the Brillouin zone. We follow the same convergence procedure as the previous one to determine the number of *k*-points in the first Brillouin zone. In this study, the k-point number is varied from (2×2×1) (2 points) to 5×5×3 (24 points). For each value, the total energy is calculated.

For the compounds $AGaS_2$ *(A=K, Rb, Cs),* the converged total energy is obtained for a 5×5×2 sampling grid of the irreducible Brillouin zone (24 points), this gives a relative variation of the total energy of the order of 10^{-9}. **Figure III.2** shows the results of this study, and **Table III.2** provides an overview of the evolution of E_{tot} versus *nKpt* for $KGaS_2$.

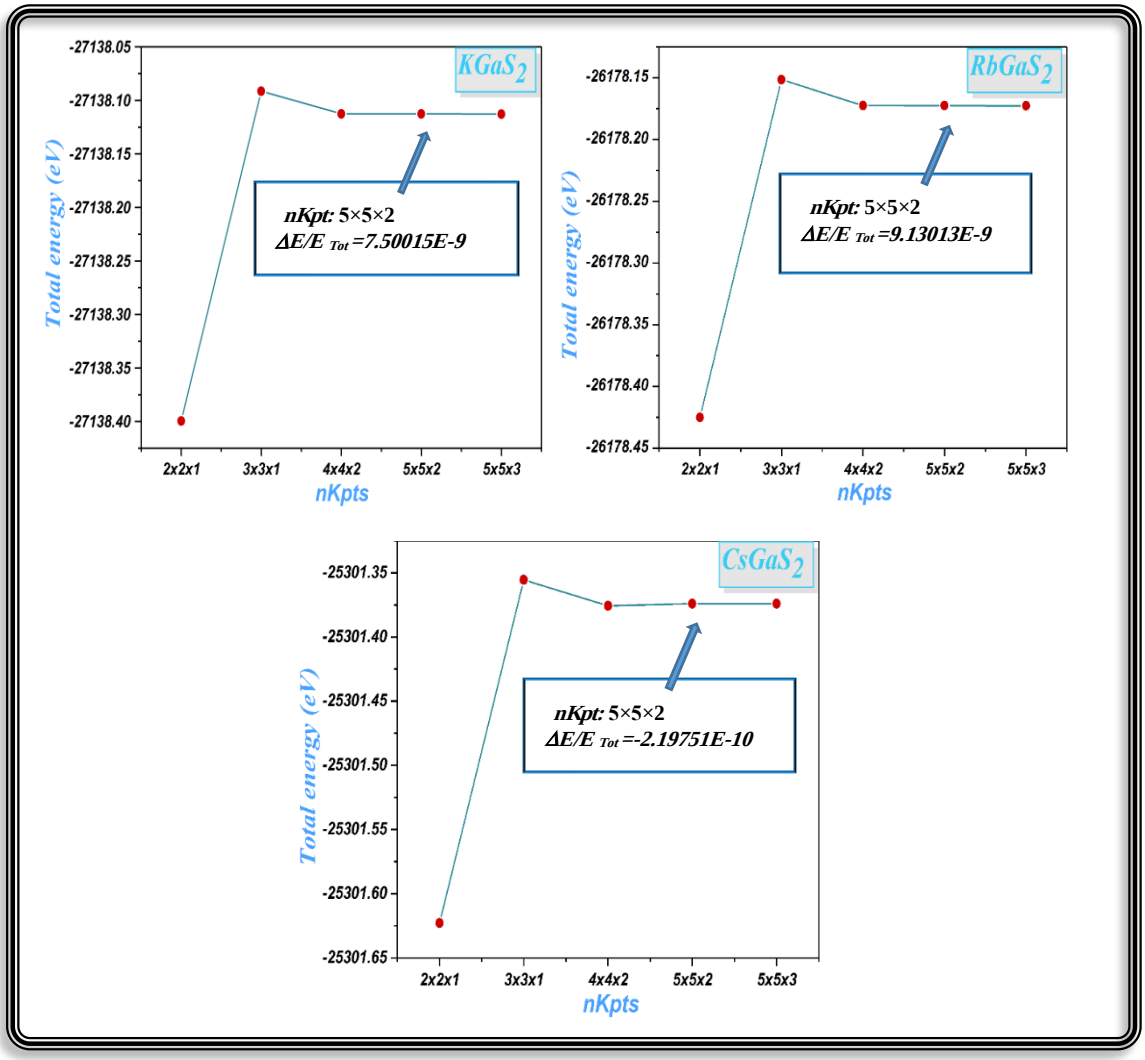

Figure III.2: *Convergence of the total energy as a function of nkpt for compounds $AGaS_2$ (A=K, Rb, Cs).*

Table III.2: *Convergence total energy as a function of k-points, for compound $AGaS_2$ (A=K, Rb, Cs) E_{cut}=450 eV.*

$KGaS_2$		
k-points	***Total Energy (eV)***	$\Delta E/E_{tot}$
2×2×1	-27138.39956	-1.05658E-5
3×3×1	-27138.09134	7.91568E-7
4×4×2	-27138.11261	7.75109E-9
5×5×2	**-27138.11262**	**7.50015E-9**
5×5×3	-27138.11282	0

III.4 Structural properties

Determining the ground state equilibrium geometry including unit cell parameters and atomic coordinates is the first important step in obtaining the physical properties of a given material on a microscopic scale. Nowadays, it is possible to calculate the total energy of solids fairly accurately using certain approximations such as GGA.

After testing the convergence parameters (E_{cut} and *k*-point), we proceed to optimize the equilibrium geometry by relaxing the unit cell parameters and the atomic positions (i.e. minimizing the components of the forces exerted on each atom). Indeed, the Hellmann–Feynman forces acting on each ion vanish when the total energy reaches its minimum. CASTEP uses the *Fletcher-Goldfarb-Shanno* "BFGS" algorithm, which is a fast, yet accurate self-consistent minimization scheme [4]. Both unit cell parameters and atomic coordinates are allowed to relax using the following convergence criteria**:**

- Maximal forces is: 0.01 eV/Å.
- Tolerance in energy is: 5.0×10^{-6} eV/atom.
- Maximum displacement is: 5.0×10^{-4} Å.
- Maximum stress is: 0.02 *GPa*.

The obtained results for the three materials are reported in **Tables III.3, 4, 5** and **6** along with their experimental counterpart. What is interesting in the data obtained in this study by the GGA-PBE approximation is the fairly good agreement with the experimental values. This demonstrates the reliability of the employed calculation

methodology and gives confidence on the subsequent calculated electronic and optical properties.

Table III.3: *Calculated (Cal) and Experimental (Exp) structural parameters: cell parameters (a, b, c and β), volume (V), and density (ρ) for $KGaS_2$, $RbGaS_2$ and $CsGaS_2$*

System		$KGaS_2$		$RbGaS_2$		$CsGaS_2$	
Chemical name		Potassium Gallium Sulfide		Rubidium Gallium Sulfide		Cesium Gallium Sulfide	
Space group, Z		C 2/c, 15		C 2/c, 15		C 2/c, 15	
Symmetry		Monoclinic		Monoclinic		Monoclinic	
		$KGaS_2$		$RbGaS_2$		$CsGaS_2$	
		Cal	Exp[a]	Cal	Exp[b]	Cal	Exp[c]
Unit cell Parameters	a (Å)	10.56680	10.42500	10.68070	10.48400	10.82910	10.57170
	b (Å)	10.57140	10.44240	10.67760	10.46800	10.82920	10.57070
	c (Å)	14.90520	14.79100	15.59800	15.39000	16.35910	16.08700
	a/c	0.70893	0.70482	0.68474	0.68122	0.66196	0.65715
	b/c	0.70924	0.70599	0.68454	0.68018	0.66196	0.66196
	β (°)	100.2300	100.1600	99.8556	99.6900	99.5277	99.4449
Cell volume	V (Å³)	1638.52938	1584.92897	1752.61010	1664.90176	1891.976052	1773.356311
Density	ρ (g/cm³)	2.80442	2.89926	3.32482	3.49998	3.74606	3.99660

a: [5]; b: [6]; c: [7].

Table III.4: *Calculated (Cal) and Experimental (Exp) atomic coordinates (x, y, z) for $KGaS_2$ and site (Wyckoff position " P. W ").*

Atom	X		Y		Z		SITE
	Cal	Exp	Cal	Exp	Cal	Exp	
K K1	0.46433	0.46500	0.31251	0.31200	0.11026	0.10900	8f
K K2	0.28474	0.28500	0.06180	0.06300	0.38835	0.39000	8f
Ga Ga1	0.10172	0.10200	0.18926	0.18900	0.16289	0.16300	8f
Ga Ga2	0.14510	0.14500	0.43596	0.43600	0.33746	0.33800	8f
S S1	0.00000	0.00000	0.05739	0.06000	0.25000	0.25000	8f
S S2	0.00000	0.00000	0.56762	0.57000	0.25000	0.25000	8f
S S3	0.20530	0.19900	0.06295	0.06200	0.07063	0.07600	8f
S S4	0.25529	0.25500	0.31238	0.31000	0.25049	0.25000	4e
S S5	0.04508	0.04500	0.31287	0.31300	0.43290	0.43200	4e

Table III.5: *Calculated (Cal) and Experimental (Exp) atomic coordinates (x, y, z) for $RbGaS_2$ and site (Wyckoff position " P.W ").*

Atom	X		Y		Z		SITE
	Cal	Exp	Cal	Exp	Cal	Exp	
Rb Rb1	0.46373	0.46320	0.18737	0.18740	0.10640	0.10620	8f
Rb Rb2	0.28575	0.28580	0.43799	0.43850	0.39370	0.39520	8f
Ga Ga1	0.10267	0.10270	0.31050	0.31060	0.16776	0.16740	8f
Ga Ga2	0.14358	0.14380	0.06429	0.06420	0.33255	0.33280	8f
S S1	0.25359	0.25420	0.18744	0.18780	0.25031	0.25020	8f
S S2	0.20763	0.20800	0.43713	0.43750	0.08014	0.08000	8f
S S3	0.00000	0.00000	0.44099	0.44260	0.25000	0.25000	8f
S S4	0.50000	0.50000	0.43392	0.43240	0.25000	0.25000	4e
S S5	0.04297	0.04360	0.18733	0.18770	0.42394	0.42390	4e

Table III.6: *Calculated (Cal) and Experimental (Exp) atomic coordinates (x, y, z) for $CsGaS_2$ and site (Wyckoff position " P.W ").*

Atom	X		Y		Z		SITE
	Cal	Exp	Cal	Exp	Cal	Exp	
Cs Cs1	0.28686	0.28710	0.06178	0.06210	0.39860	0.39970	8f
Cs Cs2	0.46320	0.46290	0.31240	0.31260	0.10347	0.10260	8f
Ga Ga1	0.10337	0.10390	0.29310	0.18920	0.17240	0.17190	8f
Ga Ga2	0.14201	0.14270	0.57840	0.43570	0.32797	0.32830	8f
S S1	0.04088	0.04070	0.35300	0.31230	0.41517	0.41510	8f
S S2	0.20999	0.20970	0.27250	0.06280	0.08991	0.08900	8f
S S3	0.25115	0.25270	0.31219	0.31230	0.25036	0.25030	8f
S S4	0.00000	0.00000	0.06115	0.05980	0.25000	0.25000	4e
S S5	0.00000	0.00000	0.56326	0.56490	0.25000	0.25000	4e

III.5 Electronic properties

The study of electronic properties is of particular importance because they allow us to analyse and understand the nature of the bonds that form between the different elements of any material. These properties include electronic band structure, total and orbital projected density state. In this work, the study of the electronic properties was carried out using the GGA-PBE approximation with a denser non shifted *k* points sampling grid of (10 ×10×5), which corresponds to 140 points for a sampling step of 0.0123 $Å^{-1}$.

III.5.1 Structure of the energy bands

The solid state electron band structure reveals the eigenvalues associated with conduction and valence bands along specific directions in the Brillouin zone of a particular crystal structure. One of the most important reasons for calculating the electronic band structure is to determine the band gap (the energy gap). That is to say, in the Khon-Sham approach the difference between the highest allowed valence band energy and the lowest allowed conduction band energy, as this can give an idea on the potential uses for optical device applications. Moreover, the calculated electronic band structure allows us to determine the type of the compound (metal, insulator, or semiconductor).

Figure III.3, shows the first Brillouin zone and the corresponding high symmetry points of the herein considered monoclinic lattice (C 2/c); L(-1/2,0,1/2), M(-1/2,-1/2,1/2), A (-1/2,0,0), G (0,0,0), Z(0,-1/2,1/2) and V(0,0,1/2). **Figure III.4**. Shows the corresponding electronic band structure as calculated using GGA-PBE approximation along the high symmetry directions.

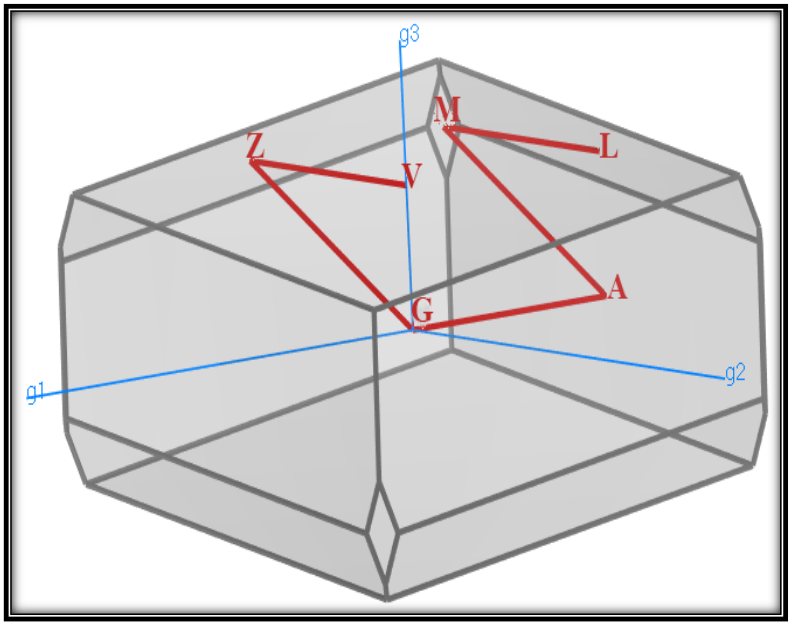

Figure III.3: *First Brillouin zone for the monoclinic lattice (*C 2/c*) and the points of high symmetry. (g1, g2 and g3 the vectors of the reciprocal lattice).*

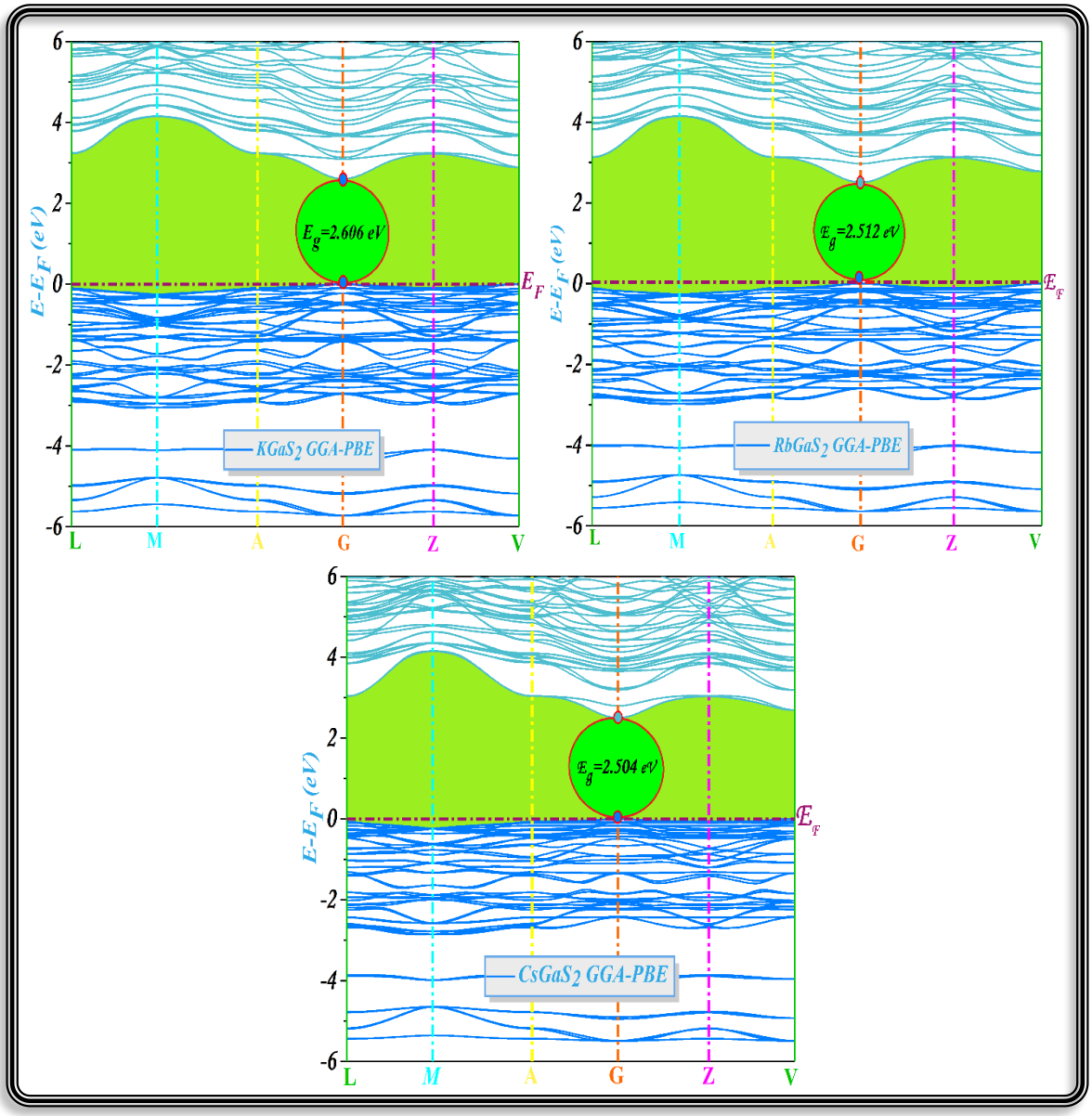

Figure III.4: *Energy band structures of calculated by GGA-PBE. The Fermi level is set at 0 eV and marked by the dashed violet horizontal line.*

From **Figure III.4**, one can note that the three materials ($KGaS_2$, $RbGaS_2$, $CsGaS_2$) have direct band gaps by evidence of both the top of the valence band (*VB*) and the bottom of the conduction band (*CB*) which are located at the **G** -point. The calculated band gaps using the GGA-PBE are 2.606 eV, 2.512 eV and 2.504 eV for $KGaS_2$, $RbGaS_2$ and $CsGaS_2$ respectively, revealing their semiconducting nature. The flat valance band character and the highly dispersive conduction bands are a clear indication of the high mobility of electrons compared to that of holes. This suggests better transport performance for n type doping of the herein considered materials.

III.5.2 Density of states

Once the DFT calculations have been performed, the electronic density of states (DOS) can be determined by integrating the resulting electron density in k-space.

The DOS shows both the occupied and unoccupied available states, a high DOS at a specific energy level means that there are many states available for occupation. A DOS of zero means that no state can be occupied at this energy level. DOS is often used for a quick visual analysis of the electronic structure. Characteristics such as the width of the valence band, the energy gap and the number and intensity of the main features are helpful in qualitatively interpreting experimental spectroscopic data. The importance of the density of states can be found also in the calculation of the speed of any process in a solid, from the diffusion of an electron to the absorption and emission of light.

DOS is provided with two analysis tools, namely, the total density of states (TDOS) and the partial density of state (PDOS). TDOS presents, in the form of a histogram, the number of mono-electronic states according to energy. PDOS are based on the analysis of Mulliken populations and carried out by projection of mono-electronic orbitals on a basis of atomic orbitals located around the different nuclei of the mesh.

TDOS and PDOS corresponding to the energy bands of the $KGaS_2$, $RbGaS_2$ and $CsGaS_2$ compounds are calculated. This allows one to obtain information regarding the orbital character of the electronic states and the chemical bonding. The obtained results are depicted in **Figure III.5**.

One can clearly observe the existence of six important regions, five regions of the valence band (*V1*, *V2*, *V3*, *V4*, *V5*) mainly located between -15 eV up to Fermi level (E_F), and the last one, namely (*C*) at the conduction band. The first region is represented by the valence band group *V1*, which lays approximately from -3 eV up to Fermi level (E_F), is completely dominated by the S-3p states with a small contribution from the *Ga-4p* states. The second group *V2*, located in the energy range from -5.85 to -3.91 eV is an admixture of the *S-3p* and *Ga-4s* states. The third group (*V3*) is predominately occupied by the alkali metal *p* states. This group charges its position drastically according to the nature of the alkali atom, it shifts more and more towards the Fermi level when going down the periodic table from *K* to *Cs* . The fourth valence band group *V4*, which spreads approximately from -13 to -11.74 eV, is mainly due to the *S-3p*

orbitals. The lowest energy group *V5*, which is stretched from approximately −10.6 to −9.9 eV, is formed of the *Ga-3d* states with a very small contribution from the *S-3s*.

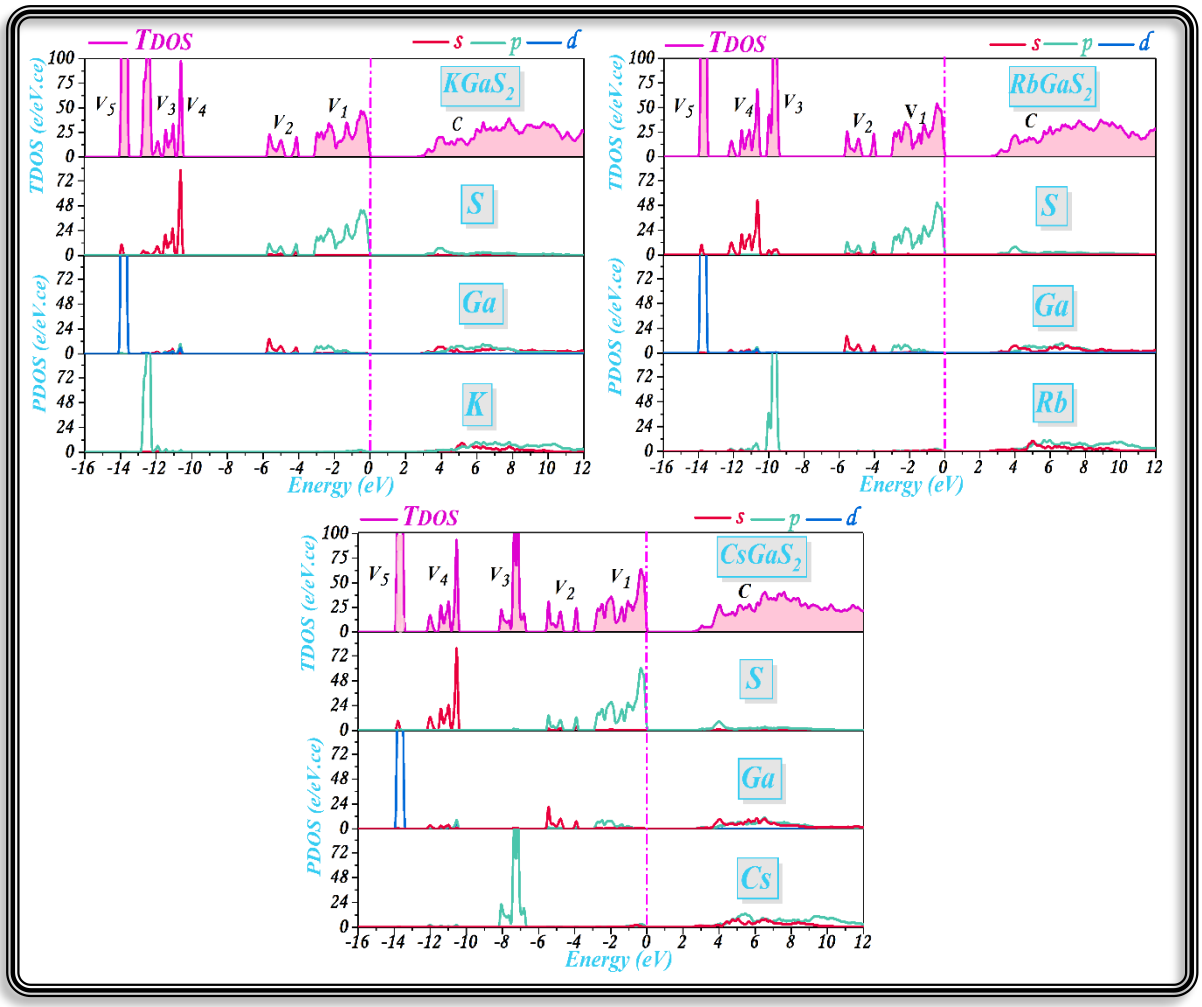

Figure III.5: *Total and partial density of states for the $AGaS_2$ (A=K, Rb, Cs) compounds.*

III.5.3 Mulliken population analysis

The Mulliken populations can serve as a means of describing the electronic distribution in an atomic or molecular system. In the CASTEP code, Mulliken population analysis is performed using a projection of plane wave states on a localized basis using a technique described by Sanchez-Portail (*1995*) [8].

The ionic character of a material may be related to the charge transfer between its respective cations and the anions constituents. In order to explore the chemical bonding character of the *AGaS2 (A=K, Rb, Cs)* compounds we calculated the transferred charge between cations and anions based on the Mulliken population analysis. A high value of

the bond population indicates a covalent bond, while a low value indicates an ionic bond. The obtained atomic charges are shown in Table III.7.

Table III.7: *Mulliken atomic charges of $AGaS_2$ (A=K, Rb, Cs) compounds.*

	Charges (e)		
Atom	$KGaS_2$	$RbGaS_2$	$CsGaS_2$
A	0.79	0.83	0.99
Ga	0.55	0.49	0.44
S	-0.69	-0.69	-0.69

From the table we can conclude the following:

- For $KGaS_2$ each atom K loses approximately $0.79\ e$ and each atom of *Ga* loses also $0.55\ e$ and *S* receives $-0.69\ e$ $(-0.35e \times 2)$ of the total charge transferred by the atoms of *K* and *Ga*.
- For $RbGaS_2$, *Rb* transfers a charge of $0.83\ e$ and *Ga* transfers 0.49 where *S* receives $-0.69\ e$ $(-0.35e \times 2)$.
- In the case of $CsGaS_2$, *Cs* and *Ga* transfer $0.99\ e$, $0.44\ e$ respectively where *S* receives $-0.69\ e(-0.35e \times 2)$.

It is noted here that the sulfur atoms *S* lack two electrons so that their outer shell (the valence shell) are complete, on the other hand the atoms *A* (*K, Rb, Cs*) and *Ga* have respectively one and three electrons in their outermost electronic shell. Thus, the herein considered materials must have the formal valence state $A^{+}Ga^{+3}(S^{-2})_2$ if we consider the extreme case of total charge transfer between the different constituents. Our results give the effective valence states $K^{+0.79}\,Ga^{+0.55}(S^{-0.35})_2$, $Rb^{+0.83}Ga^{+0.49}(S^{-0.35})_2$ and $Cs^{+0.99}Ga^{+0.44}\,(S^{-0.35})_2$ .Therefore, from these results, we deduce that the bonds of $KGaS_2$, $RbGaS_2$ and $CsGaS_2$ are not purely ionic but have certain degree of covalence.

Table III.8 gives an idea of the interactions between the electronic populations of atomic bonds in the herein considered materials. It can be seen that there is a strong charge transfer between the caesium *A* atoms and the sulfur *S* atoms giving evidence for the strong ionic character of the *A-S* bond .However, according to Figure III.6, the population of the *Ga-S* bond indicates the low covalent character of this bond in $KGaS_2$, $RbGaS_2$ and $CsGaS_2$. The negative populations of the *A-Ga* bond (*A = K or Rb*) is a clear indication of the anti-binding interaction between these two populations, but the

populations of the *Cs-Ga* bond is a clear indication of the binding interaction between these two populations.

Table III.8: *Interatomic distances (Å) for the $AGaS_2$ (A=K, Rb, Cs) compounds.*

System	Bond	Distance (Å)	M. P
$KGaS_2$	**K-Ga**	3.81247	-0.57
	Ga-S	2.29761	0.62
	K-S	3.20539	0.08
$RbGaS_2$	**Rb-Ga**	3.93198	-0.58
	Ga-S	2.26223	0.66
	Rb-S	3.31947	0.07
$CsGaS_2$	**Cs-Ga**	3.65959	0.08
	Ga-S	2.29599	0.64
	Cs-S	3.56992	0.10

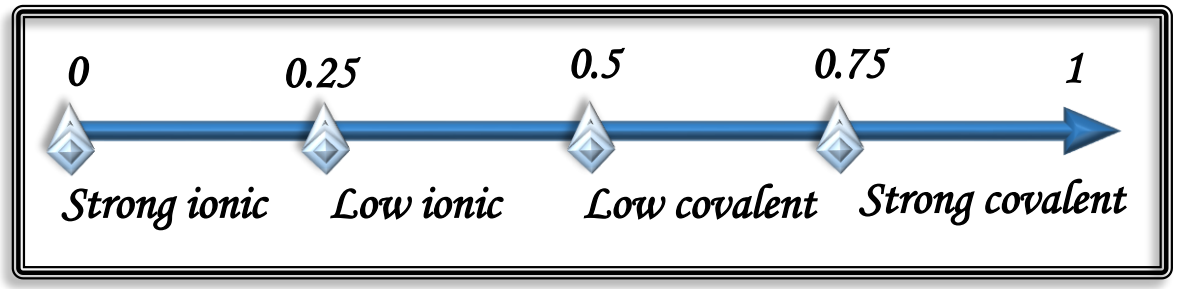

Figure III.6: *Classification of the nature of the bonds according to Mulliken population analysis.*

III.6 Optical properties

It is of great interest to know the different ways in which light interacts with matter in solid state physics, for example absorption, transmission, reflection, scattering and emission. Studying the optical properties of solids has proven to be a powerful tool in our understanding of the electronic properties of materials.

In particular, structures in the energy dependence of the properties mentioned above is very great. Crucial information on eigenvalues and Eigen functions is necessary to calculate the frequency/energy dependent optical response functions.

Calculations of the optical properties require more *k*-points than ordinary self-consistent field calculations; a 10×10×5 *k*-points grid is used in the present work. It is well known, that many low symmetry crystals display varying degree of optical

anisotropy. For this reason, the optical functions of the considered crystals are calculated for polarized incident radiation with electric field vector $\vec{E}$ parallel to the principal crystallographic axes $\vec{E}//[100], \vec{E}//[010]$ and $\vec{E}//[001]$ for the [0-15 eV] energy range.

- In the linear response range, the optical properties of a matter can be characterized by an understanding of response functions such as the complex dielectric coefficient $\varepsilon(\omega) = \varepsilon_1(\omega) + i\varepsilon_2(\omega)$ [9].with $\varepsilon_2(\omega)$ being the imaginary component of the complex dielectric coefficient; it is related to absorption and describes the energy losses that occur in a medium due to electronic transitions. $\varepsilon_2(\omega)$ can be calculated with the momentum matrix elements between the occupied and unoccupied wave functions within the selection rules:

$$\varepsilon_2(\omega) = \frac{2\pi e^2}{m_e^2\omega^2\varepsilon_0}\sum_{c,v}\int_{BZ}|\langle\Psi_k^c|\vec{u}.\vec{r}|\Psi_k^v\rangle|^2\delta(E_k^c - E_k^v - \hbar\omega)d\vec{k} \qquad \textbf{(III.1)}$$

Where ω is the light frequency, *e* is the electronic charge, $\vec{u}$ is the vector defining the polarization of the incident electric field, Ψ_k^c and Ψ_k^v are the conduction and valence band wave functions at k, respectively.

$\varepsilon_1(\omega)$ is the real part of the dielectric function and it can be calculated from $\varepsilon_2(\omega)$ by Kramer-Kroning relations.

$$\varepsilon_1(\omega) = 1 + \frac{2}{\pi}P\int_0^\infty \frac{\acute{\omega}\varepsilon_2(\omega)}{\acute{\omega}^2-\omega^2}d\acute{\omega} \qquad \textbf{(III.2)}$$

Where *P* represents the main integral.

All the other energy dependant optical constants can be derived from $\varepsilon_1(\omega)$ and $\varepsilon_2(\omega)$ this includes the refractive index, the extinction coefficient, the absorption coefficient, and the reflectivity.

The absorptive $\varepsilon_2(\omega)$ and dispersive $\varepsilon_1(\omega)$ parts of the dielectric function as functions of the photon energy for three polarizations of the electric field $\vec{E}$ of the incident light with respect to the crystallographic axes $\vec{E}//[100], \vec{E}//[010]$ and $\vec{E}//[001]$ for the $AGaS_2$ *(A=K, Rb, Cs)* compounds are shown in **Figure III.7**.

All three materials show similar energy dependant optical response functions. This is mainly due to their similar electronic band structures. Moreover, their optical reposes indicate high optical anisotropy in the visible and in the lower energy part of the UV spectrum by evidence the spectrum peculiarities, which highly depend on the polarisation of the electromagnetic radiation.

The absorptive part $\varepsilon_2(\omega)$ [see **Figure III.7 (*a*)**] of the dielectric function $\varepsilon(\omega)$ of these materials exhibits tow structures labelled *A*, *B*. Those peaks are mostly due to direct electronic transitions from the occupied valence bands to the allowed unoccupied states in the conduction band. *A* is centred at 4.79 eV for $\vec{E}//[100]$and 4.44 eV for $\vec{E}//[001]$ of $KGaS_2$, and of $RbGaS_2$ ($CsGaS_2$) is 4.69 eV (4.50 eV) for $\vec{E}//[100]$and 4.44 eV (4.43 eV) for $\vec{E}//[001]$. *B* is centred at approximately 6.56 eV for $\vec{E}//[100]$and 6.50 eV for $\vec{E}//[001]$ of $KGaS_2$, and of $RbGaS_2$ ($CsGaS_2$) is 6.90eV (6.74 eV) for $\vec{E}//[100]$ and 6.24 eV (6.14 eV) for $\vec{E}//[001]$ [see **Figure III.5**].

The static dielectric constant $\varepsilon_1(0) = \varepsilon_1(\omega \to 0)$ defined as the zero frequency limit of the real part of the dielectric function, is the most important quantity in the $\varepsilon_1(\omega)$ spectrum [see **Figure III.7 (*b*)**].The calculated value of $\varepsilon_1(0)$ for $KGaS_2$ ($RbGaS_2$ and $CsGaS_2$) is equal to 4.92 (4.73 and 4.76), for $\vec{E}//[100]$and 4.68 (4.61 and 4.64) for $\vec{E}//[001]$, ince $\varepsilon_1(0)$ increases with decreasing band gap.

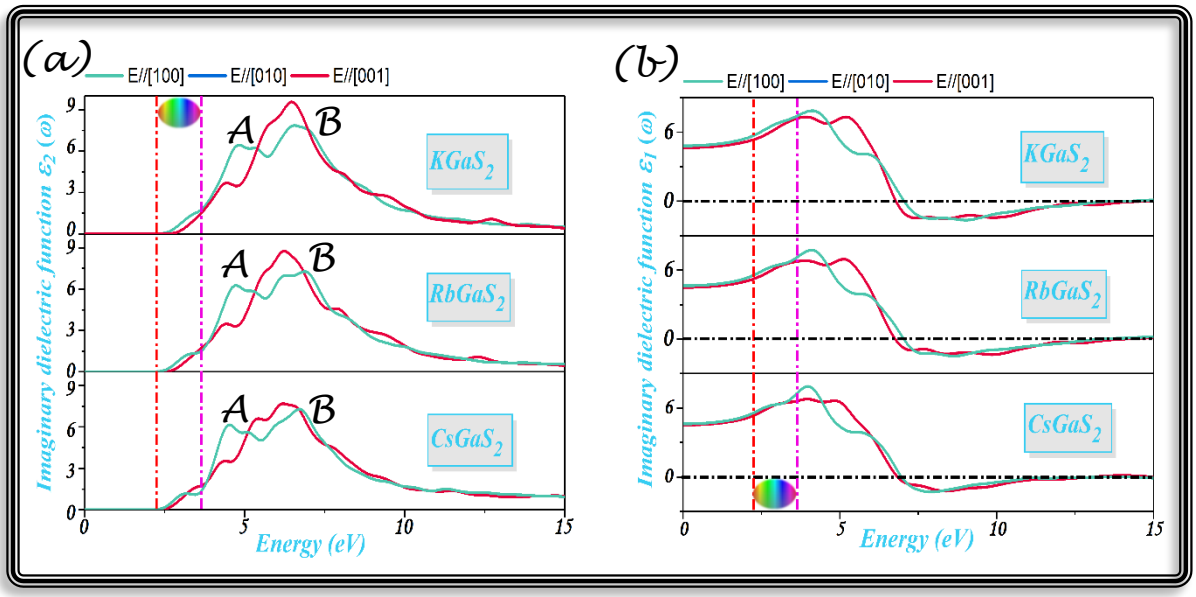

Figure III.7: *Calculated (a) imaginary part $\varepsilon_2(\omega)$ and (b) real part $\varepsilon_1(\omega)$ of the dielectric function for the $AGaS_2$ (A=K, Rb, Cs) compounds.*

❖ The complex refractive index is related to the complex dielectric function via:

$$N(\omega) = \sqrt{\varepsilon(\omega)} \qquad \textbf{(III.3)}$$

Given that $N(\omega)$is written as:

$$N(\omega) = n(\omega) + ik(\omega) \qquad \textbf{(III.4)}$$

Where $n(\omega)$ is the refractive index, and $k(\omega)$ the extinction coefficient.

The real and imaginary components of both the refractive index and the dielectric function are therefore related by:

$$n(\omega) = \frac{1}{\sqrt{2}}\left[(\varepsilon_1^2(\omega) + \varepsilon_2^2(\omega))^{1/2} + \varepsilon_1(\omega)\right]^{1/2} \quad \textbf{(III.5)}$$

$$k(\omega) = \frac{1}{\sqrt{2}}\left[(\varepsilon_1^2(\omega) + \varepsilon_2^2(\omega))^{1/2} - \varepsilon_1(\omega)\right]^{1/2} \quad \textbf{(III.6)}$$

One of the most important optical constants is the refractive index, which in general depends on the wavelength of the electromagnetic wave, by a ratio called the dispersion. The case where an electromagnetic wave can lose its energy during its propagation, the refractive index becomes complex. The real part is usually the index of refraction *n*, and the imaginary part is called the extinction coefficient *k*.

The calculated refractive index spectra of the $AGaS_2$ (*A=K, Rb, Cs*) compounds are shown in **Figure III.8 (*a*)**. The static refractive index $n(0)$ (the refractive index at zero energy) of the $KGaS_2$ is equal to 2.24, and $RbGaS_2$ ($CsGaS_2$) is 2.19 (2.16) for $\vec{E}//[100]$ and 2.17, 2.13(2.13) for $\vec{E}//[001]$ respectively. The extinction coefficient in the visible region [see **Figure III.8 (*b*)**] increases to get a maximum value at the UV spectrum when for $\vec{E}//[100]$ ($\vec{E}//[001]$).

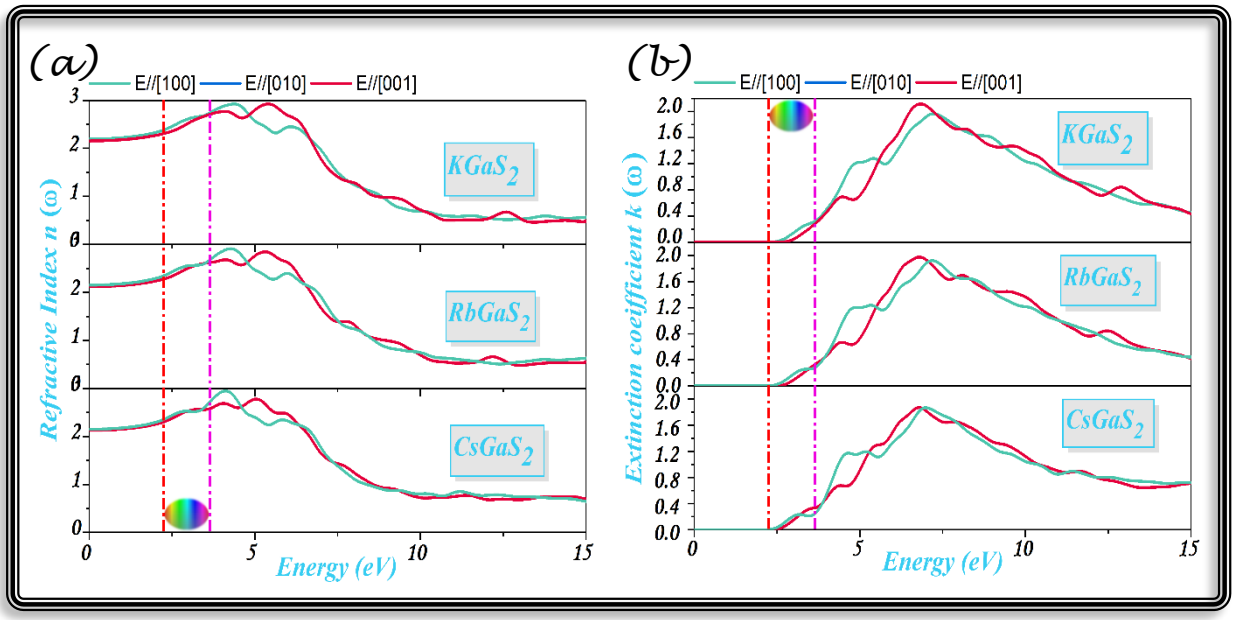

Figure III.8: *(a) The refractive index $n(\omega)$ and (b) the extinction $k(\omega)$ spectrums for the $AGaS_2$ (A=K, Rb, Cs) compounds.*

- The optical absorption $\alpha(\omega)$ can be calculated from $\varepsilon_1(\omega)$ and $\varepsilon_2(\omega)$as follows:

$$\alpha(\omega) = \sqrt{2}\omega\left[(\varepsilon_1^2(\omega) + \varepsilon_2^2(\omega))^{1/2} - \varepsilon_1(\omega)\right]^{1/2} \qquad \textbf{(III.7)}$$

The absorption coefficient $\alpha(\omega)$ is a basic way to measure how far light with a specific energy can penetrate a material before being absorbed. The absorption coefficient depends on the incident photon energy and expresses the ratio between the number of photons actually absorbed by the crystal per unit volume per second and the number of incident photons per unit area per second. From the point of view of the structure of electron bands, we are interested in the probability that, under the influence of the radiation field, an electron makes a transition between two energy levels. **Figure III.9** shows the optical absorption spectra of the $AGaS_2$ (*A=K, Rb, Cs*) compounds, in which the fundamental absorption edge starts approximately at 2.64 eV, 2.76 eV and 2.70 eV for $\vec{E}//[001]$ and 3.10 eV, 2.91 eV and 2.78 eV for $\vec{E}//[100]$ in $KGaS_2$, $RbGaS_2$ and $CsGaS_2$ respectively. The absorption coefficient increases with increasing photon energy, reaching a maximum and then decreasing to reach its minimum. The absorption spectrum shows some peaks that can be explained by the inter-band transitions using the band structure results. The $KGaS_2$, $RbGaS_2$ and $CsGaS_2$ compounds can be used as an absorptive layer in the energy range from 2.64 to$>$ 15 eV. The investigated materials exhibits noticeable absorption in the visible ultraviolet range.

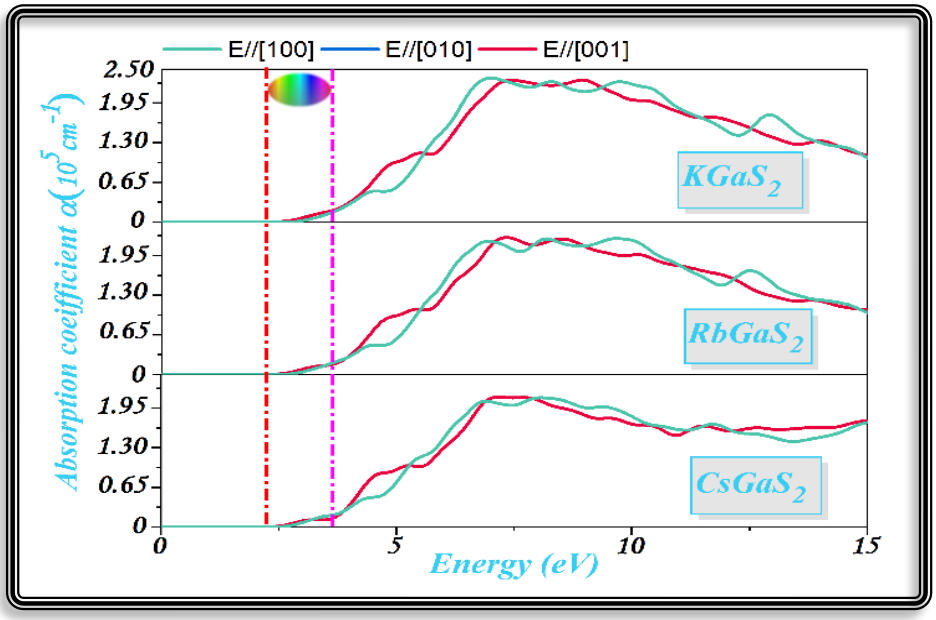

Figure III.9: *Linear absorption $\alpha(\omega)$ spectrum of $AGaS_2$ (A=K, Rb, Cs) compounds.*

III.7 Coclusion

In this chapter, we have calculated the structural, electronic and optical properties of $AGaS_2$ *(A=K, Rb, Cs)* compounds by the GGA approximation using the plane wave pseudo-potential method with as implemented in the CASTEP package.

A summary of our results is as follows:

- The structural properties (structural parameters and atomic positions) are in good agreement with the available experimental data.
- The calculated electronic band structure and density of states show that the $AGaS_2$ *(A=K, Rb, Cs)* are indirect moderate band gap semiconductors.
- Many energy dependant optical response functions, namely the complex dielectric function and refractive index, the optical absorption, where calculated and discussed. The obtained results show that the $AGaS_2$ *(A=K, Rb, Cs)* compounds possess a high absorption band in the UV region.

References

[1] Vanderbilt, D., Soft self-consistent pseudopotentials in a generalized eigenvalue formalism. Physical review B, 1990. 41(11): p. 7892.

[2] Benmakhlouf, A., et al., Structural, electronic and magnetic properties of the manganese telluride layers AMnTe2 (A= K, Rb, Cs) from first-principles calculations. Journal of Magnetism and Magnetic Materials, 2018. 465: p. 430-436.

[3] Monkhorst, H.J. and J.D. Pack, Special points for Brillouin-zone integrations. Physical review B, 1976. 13(12): p. 5188.

[4] Fischer, T.H. and J. Almlof, General methods for geometry and wave function optimization. The Journal of Physical Chemistry, 1992. 96(24): p. 9768-9774.

[5] Delgado, G., et al., *Growth and crystal structure of the layered compound TlGaSe2*. Crystal Research and Technology: Journal of Experimental and Industrial Crystallography, 2007. 42(7): p. 663-666.

[6] Kumari, A. and K. Vidyasagar, *Rubidium thiogallate*. Acta Crystallographica Section E: Structure Reports Online, 2005. 61(9): p. i193-i195

[7] Friedrich, D., et al., Polymorphism of CsGaS 2–structural characterization of a new two-dimensional polymorph and study of the phase-transition kinetics. Inorganic Chemistry Frontiers, 2017. 4(2): p. 393-400.

[8] R. S. Mulliken, J. Chem. Phys., (1955), vol 23, no 10, p 1833

[9] Tasker, P., The stability of ionic crystal surfaces. Journal of Physics C: Solid State Physics, 1979. 12(22): p. 4977.

General Conclusion

General conclusion

In the present study, the structural, electronic and optical properties of the $AGaS_2$ *(A=K, Rb, Cs)* compounds have been studied. The plane wave ultra-soft pseudo-potential methods and the generalized gradient approximation (GGA) have been used to describe the exchange-correlation energy within the density-functional theory as implemented in the CASTEP code.

In order to describe the fundamental state of the considered system, we first studied the structural properties. The obtained results (structural parameters and atomic positions) are in good agreement with the available experimental data.

Also, the electronic properties such as band structures and density of states have been presented. The $AGaS_2$ *(A=K, Rb, Cs)* compounds are direct moderate band gaps semiconductors by evidence of the valence band (*VB*) maximum and the conduction band (*CB*) minimum at gamma point. The calculated band gaps are about 2.606 eV, 2.512 eV and 2.504 eV for $KGaS_2$, $RbGaS_2$ and $CsGaS_2$ respectively. Mulliken charges analysis and band populations for this systems give evidence for the strong ionic character of the A-S bond, and the covalent character of the *Ga-S* bond.

In order to study the optical response of the $KGaS_2$, $RbGaS_2$ and $CsGaS_2$ semiconductors versus incident light, the optical properties such as dielectric function and absorption coefficient, refractive and the extinction coefficient have been also calculated. The static dielectric constants $\varepsilon(0)$ and refractive index $n(0)$ have been estimated, for the [100], [010] and [001] polarizations. Our study show that the $AGaS_2$ *(A=K, Rb, Cs)* compounds show a somewhat high extent of optical anisotropy in in the photon energy range 0-15 eV. The obtained results show that both compounds are active in the extreme UV region.

Finally, from our short experiences using the CASTEP code it turns out that this program is a very powerful code, which allows direct and easy calculation of the electronic structures and the optical properties of crystals.

ملخص

نقدم هنا ملخصا لنتائج دراسة أجريت على الخصائص البنيوية، الالكترونية و البصرية لمركبات الكالكوجين ذات الصيغة $AGaS_2$ $(A=K, Rb, Cs)$ في الطور الأحادي الميل باستعمال المبادئ الأولية لميكانيكا الكم. هذا وقد اتخذنا من نظرية دالية الكثافة وتقريب التدرج المعمم لطاقة التبادل والارتباط ومن منهج الأمواج المستوية والمكونات المستعارة سبيلا لذلك. كانت النتائج المحصلة على توافق جيد مع المعطيات المتوفرة عن هذه المركبات خاصة ما تعلق منها بالبنية البلورية للحالة الأساسية. كما بيَّنَتْ بنية عصبات طاقة الالكترونات ان مركبات الكالكوجين التي شملتها الدراسة، أشباه موصلات ذات فجوات طاقة مباشرة ومعتدلة نسبيا. ومن تحليل أطياف بعض من الخصائص البصرية، تَجَلَّتْ كفاءة هذه المركبات في امتصاص الاطوال الموجية القصيرة للطيف الفوق بنفسجي.

كلمات مفتاحية: نظرية دالية الكثافة، GGA, CASTEP، أنصاف النواقل، الخصائص البنيوية، الخصائص الإلكترونية، الخصائص البصرية، $KGaS_2$. $RbGaS_2$. $CsGaS_2$

Abstract

We present here the results of a first principle principle study on the structural, electronic and optical properties of $AGaS_2$ $(A=K, Rb, Cs)$ compounds using the plane wave pseudo-potential method . The exchange correlation potential was treated within the generalized gradient approximation (GGA) as implemented in the CASTEP code and expressed by the PBE functional. The equilibrium lattice parameters are in good agreement with the available experimental results. The calculated band structure show that the studied compounds are direct moderate gap semiconductors. A set of frequency dependent optical parameters were calculated including the complex dielectric function, the reflective index and the absorption coefficient. The obtained results show that the herein considered compounds are active in the UV region.

Key words : Density functional theory, GGA, CASTEP, semiconductors, structural properties, electronic properties, optical reponse. $KGaS_2$. $RbGaS_2$. $CsGaS_2$.

Résumé

Nous présentons ici les résultats d'une étude de premières principes sur les propriétés structurales, électroniques et optiques des composés $AGaS_2$ (A=K, Rb, Cs) en utilisant la méthode du pseudo-potentiel et des ondes planes. Le potentiel d'échange corrélation a été traité dans le cadre de l'approximation du gradient généralisé (GGA) telle qu'elle est mise en œuvre dans le code CASTEP et exprimée par la fonction PBE. Les paramètres de maille de l'état fondamentale sont en bon accord avec les résultats expérimentaux. Les diagrammes des bandes d'énergie montrent que les composés étudiés sont des semi-conducteurs à gap directs et modéré. Un ensemble de paramètres optiques a été calculé, y compris la fonction diélectrique complexe, l'indice de réflexion et le coefficient d'absorption dans une large bonde spectrale. Les résultats obtenus montrent que les composés étudés sont actifs dans le domain spectral qui correcpond aux UVs.

Mots clés : Théorie fonctinnelle de la densité, GGA, CASTEP, semi-conducteurs, propriétés structurales, propriétés électroniques, réponse optiques. $KGaS_2$. $RbGaS_2$. $CsGaS_2$.